Conflict, Climate and Cells: A disaggregated analysis*

Mariaflavia Harari
University of Pennsylvania

Eliana La Ferrara
Bocconi University, IGIER and LEAP

December 2017

Abstract

We conduct a disaggregated empirical analysis of civil conflict at the subnational level in Africa over 1997-2011 using a new gridded dataset. We construct an original measure of agriculture-relevant weather shocks exploiting within-year variation in weather and in crop growing season, and spatial variation in crop cover. Temporal and spatial spillovers in conflict are addressed through spatial econometric techniques. Negative shocks occurring during the growing season of local crops affect conflict incidence persistently, and local conflict spills over to neighboring cells. We use our estimates to trace the dynamic response to shocks and predict how future warming may affect violence.

Keywords: conflict, weather shocks, spatial spillovers, Africa

*We thank three anonymous referees, Santiago Beguería, Chris Blattman, Arun Chandrasekhar, Melissa Dell, and René Gommes for helpful comments; Gordon Hughes, Solomon Hsiang, and Mathias Thoenig for making available their codes; and seminar participants at MIT, Sciences Po, University of Michigan, the Stockholm Climate Economy Conference, the 2012 Fall B-WGAPE meeting, the 2013 EEA-ESEM Conference, and the Villars-Sur-Ollon Political Economy of Conflicts and Development conference. Marta Barazzetta, Barbara Biasi, Magda Biesiada, Xinzhu Chen, Emanuele Colonnelli, Nicola Fontana, Ludovica Gazzè, Selene Ghisolfi, Long Hong, Simone Lenzu, Anna Martinolli, Alessandra Palazzo, Yeayeun Park, Xuequan Peng, and Edoardo Teso provided excellent research assistance. La Ferrara acknowledges financial support from European Research Council grant ERC-2007-StG-208661. The usual disclaimer applies. Correspondence: harari@wharton.upenn.edu; eliana.laferrara@unibocconi.it.

1 Introduction

A vivid debate has emerged in recent years on the consequences that global warming and the increased frequency of extreme weather events have on aggregate scenarios. There is concern that the adverse impact of climatic changes may be more strongly felt in poorer and more politically unstable countries, such as those in Sub-Saharan Africa, where the majority of the population is dependent on rainfed agriculture. The correlation between vulnerability to weather shocks and propensity to conflict has spurred a growing amount of research trying to establish a causal link. This literature has traditionally employed cross-country panel data on precipitation and temperature to estimate how they affect the occurrence of civil war, defined based on predetermined thresholds in casualties.

In this paper we attempt to take a step further in understanding the relationship between climate and conflict by taking the analysis to a different scale. We conduct a geographically disaggregated analysis taking as units of observation 110 × 110 km subnational "cells," and we estimate the incidence of conflict as a function of weather shocks and a number of other covariates both in the cell and in neighboring areas, plus a "lag" in space and time of the endogenous variable.

Our approach contributes to the literature in two main directions. The first and most important is methodological. We construct a cell/year panel with a rich set of geo-referenced covariates. We model spatial and temporal dependence thorough state-of-the-art spatial econometrics techniques that have seldom been applied in economics. In particular, our model includes spatially and temporally autoregressive terms to account for the fact that conflict may be persistent over time, and that both the covariates and the presence of conflict may be correlated across space. This poses a number of challenges for estimation and constitutes an original contribution to the empirical conflict literature. This approach allows us to produce two novel sets of results. The first is the assessment of how persistent the effects are in space and time: persistence implies that even temporary shocks may have long-lasting effects on political instability. The second is the ability to better detect conflict spillovers across locations compared to the existing cross-country literature (e.g., Buhaug & Gleditsch, 2008).

A second contribution of our paper is that we look at climate indexed *within the year*. Because the main hypothesized (but not yet proven) channel linking weather shocks to conflict operates through shocks to agricultural incomes, we attempt to isolate the component of climate variability that is relevant for agriculture. Instead of using yearly averages, we measure climatic conditions during the growing season, which is when crops are most sensitive to unfavorable conditions. This is a data-intensive process that involves both within-year variation in the timing of shocks and spatial variation in crop cover.

An additional contribution relates to the climate indicator we employ. Most of the conflict literature has focused on precipitation or temperature.[1] We instead use a drought index, the Standardized Precipitation-Evapotranspiration Index (SPEI), that considers the joint effects of precipitation, potential evaporation, and temperature. This accounts for the fact that the impact of rainfall on the growing cycle of a plant depends on the extent to which water can be retained by the soil.

Our methodology and results can be summarized as follows. We assemble a panel dataset covering about 2,700 cells in 46 African countries from 1997 to 2011. We combine data from the Armed Conflict Location and Event Dataset (ACLED) with an original measure of growing season SPEI. Using maximum likelihood we estimate the probability that a cell experiences at least one conflict event during the year as a function of contemporaneous and lagged SPEI and spatial and temporal lags of conflict. In our benchmark specification this is conditional on cell fixed effects and country-specific year fixed effects, so that we identify changes in conflict propensity relative to a cell's historic mean and country-specific trends. We find that:

(i) There is a significant local-level relationship between agriculture-relevant shocks and conflict. According to our most conservative specification, a one standard deviation shock to SPEI during the growing season is associated with a 1.3 percentage point increase in conflict likelihood in the subsequent year, relative to the cell's historic mean. This is roughly 8 percent of the unconditional mean of the dependent variable. As a reference, a shock of such magnitude corresponds to the cell experiencing SPEI below its long-term mean by one standard deviation throughout four growing season months in a given year.

(ii) Conflict exhibits high persistence in time and space. When a cell experiences conflict, the cell itself has a 12 percentage point higher probability of experiencing it the following year, and each of its neighboring cells has a 2.3 percentage point higher probability of experiencing it during the same year.

[1] Recent exceptions include Hsiang, Meng, and Cane (2011), who employ El Niño-Southern Oscillation (ENSO); Couttenier & Soubeyran (2014), who employ the Palmer Drought Severity Index (PDSI); and Almer, Laurent-Lucchetti, and Oechslin (2017), who employ the Standardized Precipitation-Evapotranspiration Index (SPEI) as we do.

(iii) Climate outside the growing season has no effect on conflict. This suggests that the mechanism operates through low agricultural yields.

(iv) Conflict spillovers are particularly pronounced across countries. For conflicts at the border, spillovers appear stronger across ethnicities.

(v) Among the channels through which our effect may operate, the "opportunity cost" one seems most consistent with our data, as indicated by significant effects of weather shocks on rebel recruitment. We also find that ethnic cleavages and low state capacity exacerbate the impacts of weather shocks.

Before proceeding, two caveats are in order. The first is that by focusing on the role of local shocks our paper has little to say about long-term institutional causes of conflict. This does not reflect a judgment on the relative importance of the two sets of causes; it is a consequence of the scale at which we conduct our analysis. The second caveat relates to the extent to which our results can speak to the effects of climate change. The main indicator we use is based on the deviation of weather from its historical average and can to some extent capture global trends. At the same time, our analysis holds constant economic and political variables that endogenously evolve over the long run: we should thus refrain from extrapolating the results too far into the future or to contexts with ample possibilities for adaptation.

With these caveats in mind, we use cell-level projections of future temperature and precipitation in 2016 through 2050 to construct a SPEI forecast. We predict that negative SPEI shocks during the growing season will become 5.4 times more pronounced over the next 35 years. Based on our estimates, this implies that the marginal contribution of future SPEI shocks to conflict in an average cell and year during 2016 through 2050 is 1.2 percentage points, or about 7 percent of the unconditional mean.

Our work is related to three strands of literature. The first is the literature on climate and violent conflict (e.g., Miguel, Satyanath, and Foley, 2004; Ciccone, 2013). We conduct the analysis at a more disaggregated level, and we isolate the component of weather variation that occurs during the growing season. Also, differently from the above authors, who adopt an instrumental variables strategy, we estimate a reduced-form relationship - there is no reliable data that captures yearly variation in income or GDP in rural areas at the level of disaggregation that we employ.[2] Other authors have expanded the cross-country coverage (Couttenier &

[2]We have experimented with nighttime luminosity as a proxy for income, finding a negative and significant effect of climate shocks on luminosity. However, we prefer not to rely on luminosity as we are mostly interested

Soubeyran, 2014) or investigated the link between conflict and global warming (Burke et al., 2009; Buhaug, 2010; Hsiang et al., 2013). We share with this literature the acknowledgment that temperature is crucial, and indeed our SPEI measure combines data on temperature with data on precipitation. Our focus on within-country variation is shared by recent studies linking weather shocks to insurgency and protests, including Dell (2012), Vanden Eynde (2017), Jia (2014), and Madestam et al. (2013). O'Loughlin et al. (2012) also share the "grid" approach with us.[3]

A second strand of literature focuses on climate and development. Recent studies have investigated the impact of climate on economic growth (Dell, Jones, & Olken, 2012), mortality (Burgess et al., 2013; Kudamatsu, Persson & Strömberg, 2017), health (Maccini & Yang, 2009) and political institutions (Brückner & Ciccone, 2011).

The third strand of literature related to our work is that on the determinants of civil conflict.[4] Recent papers by Bazzi & Blattman (2014) and by Berman & Couttenier (2015) explore the role of external economic shocks on conflict. While we share with these authors the interest in local variation in economic shocks, we focus on internal climatic shocks as opposed to external income shocks. This difference becomes relevant when we think of policy implications to mitigate the role of shocks (e.g., weather-indexed insurance).

The remainder of the paper is organized as follows. In section 2 we present our conceptual framework and econometric methodology. In section 3 we discuss our data and provide descriptive statistics. In section 4 we present our main results and in section 5 we examine mechanisms and heterogeneous effects. Section 6 contains robustness checks, and section 7 concludes.

in rural incomes, which are poorly proxied by nighttime lights.

[3]Our geographic resolution and the conflict data sources are similar to O'Loughlin et al. (2012). However, our approach departs in several respects: (i) we disaggregate climate indicators by local growing season, defined based on the local main crop; O'Loughlin et al. conduct the analysis at the monthly level and control for growing season, which is defined ex post based on climatic characteristics; (ii) we employ cell and country $\times$ year fixed effects; (iii) we address spatial and temporal autocorrelation through spatial econometric techniques; (iv) we rely on satellite and not on station data; and (v) our geographic coverage is the entire African continent.

[4]For a comprehensive review, see Blattman & Miguel (2010). Among more recent contributions, Berman et al. (2017) share with us the disaggregated level of analysis but focus on mineral extraction.

2 Conceptual framework and methodology

2.1 Conceptual framework

The literature on the effects of economic shocks on conflict has traditionally stressed two channels (e.g., Collier & Hoeffler, 1998). On one hand, there is an "opportunity cost" effect: a negative shock to the local economy decreases the returns from labor market participation relative to fighting, making it more attractive to join a rebellion. On the other hand, the same negative shock implies that the size of the "pie" to be appropriated is lower, thus reducing the incentives to fight. The net effect is thus ambiguous, depending on, among other things, whether the shock occurs to a labor-intensive or capital-intensive sector. In our case, because African agriculture is typically labor intensive, based on Dal Bó & Dal Bó (2011) the opportunity cost effect would be predicted to prevail: negative agricultural shocks should lead to more conflict. Economic shocks may also have an additional effect, namely worsening the extent of poverty and exacerbating existing inequalities, thus fueling conflict in response to "grievances."

Fearon & Laitin (2003) propose different channels, stressing the role of state capacity and infrastructure. Economic shocks may reduce a government's tax base, weakening its ability to fight rebellion and leading to more conflict. Moreover, if shocks affect the quality of infrastructure (e.g., roads), an increase in conflict may be the result of logistical difficulties in repressing insurgents.

The way in which we construct our climate shock variable, namely focusing on weather during the agricultural growing season, allows us to isolate effects that are specific to agricultural yields and opportunity cost: if other channels were involved, we would expect to find an effect of weather throughout the year. As for tax revenues, our benchmark specification includes the interaction of country and year dummies, which capture aggregate shocks to state revenues. In section 5 we propose a discussion of competing mechanisms in light of our results.

2.2 Empirical strategy

We construct a dataset that has the structure of a raster grid: the units of observation are subnational "cells" of 1 degree of latitude $\times$ 1 degree of longitude (approximately 110 km). As for the resolution of the grid, theory is of limited help in selecting it a priori: the degree of localization of agricultural shocks and the spatial extent of conflict spillovers are ultimately empirical objects. We validate our choice of 1 degree resolution by conducting the analysis at higher and lower spatial scales (see section 6.1).

Our analysis is at the cell/year level. Our main dependent variable is *ANY EVENT*, a binary indicator for whether the cell has experienced a conflict-related episode in a given year. This variable is coded based on the ACLED dataset, discussed in section 3.1 below. We estimate three models: the first contains only exogenous regressors specific to the cell; the second includes a "spatial lag" of the exogenous regressors; the third (preferred) model also includes lags of the endogenous variable in time and space.

We focus on conflict incidence as opposed to onset or termination for two reasons. First, our specification with spatial and temporal lags of the dependent variable requires a balanced panel. Onset and termination regressions imply the loss of a large number of observations, and the resulting balanced sample would be small and hardly representative. Second, we are interested in how conflict in a cell spills over to neighbors and how such effects persist over time, something that is more naturally assessed with incidence. Nevertheless, in section 5.5 we discuss results for onset and termination. We now turn to the empirical specifications of the three models we estimate.

Model I

Consider a panel of N cells and T years. Denote with C a generic climate indicator (e.g., precipitation) and with GS_C the climate indicator measured in the cell-specific growing season. Let X be a vector of time-invariant controls (e.g., terrain characteristics) and γ and μ denote year and country fixed effects, respectively. Model I takes the form:

$$ANY\ EVENT_{c,i,t} = \alpha + \sum_{k=0}^{2} \beta_{1k} C_{c,t-k} + \sum_{k=0}^{2} \beta_{2k} GS\_C_{c,t-k} + \delta X_c + \gamma_t + \mu_i \tau + \varepsilon_{c,i,t} \tag{1}$$

where c denotes the cell, i the country, and t the year, and τ is a linear time trend.[5] We fit a linear probability model and estimate (1) via OLS, as it can be easily integrated with spatial econometrics techniques.

Most empirical work on conflict assumes that observations are independent across space. We instead estimate Model I following the procedure of Hsiang (2010) to adjust standard errors for both spatial and serial correlation.[6] This is appropriate in cases in which spatial correlation is

[5]For defining country fixed effects each cell is assigned to one country. Cells shared among more than one country are assigned to the country that has the largest share of the cell's territory. A "shared" dummy is included among the controls.

[6]Hsiang (2010) extends to panel data the correction originally proposed by Conley (1999) for the cross-

present in the error term ("spatial error model") but it does not model spatial dependence in the process itself. However, we expect spatial correlation both in the covariates - e.g., weather - and in conflict, through direct cross-cell spillovers.

Model II

To control for spatial correlation in the covariates, we include spatial lags of the variables of interest. The structure of spatial dependence is defined by a symmetric weighting matrix W, and the spatial lag of a variable is obtained by multiplying the matrix W by the vector of observations. Let C_t and GS_C_t be N-dimensional vectors of climate observations in year t, and let X be the matrix of cell-level controls. We estimate the following spatial Durbin model (Anselin, 1988):

$$\begin{aligned} ANY\ EVENT_{c,i,t} = \alpha + \sum_{k=0}^{2} \beta_{1k} C_{c,t-k} + \sum_{k=0}^{2} \beta_{2k} GS\_C_{c,t-k} + \delta X_c + \mu_i \tau + \\ + \sum_{k=0}^{2} \theta_{1k} W \cdot C_{t-k} + \sum_{k=0}^{2} \theta_{2k} W \cdot GS\_C_{t-k} + \lambda W \cdot X + W \cdot \mu\tau + \gamma_t + \varepsilon_{c,i,t} \end{aligned} \tag{2}$$

Our benchmark W is a binary contiguity matrix in which a weight of 1 is assigned to cells surrounding the cell of interest - within a 180 km distance cutoff - and a weight of 0 to other cells. This implies that we effectively consider as neighbors the eight bordering cells. In section 6.1 we conduct a sensitivity analysis to different spatial matrices. For ease of interpretation we do not row-standardize W, so the coefficients on the spatial lags, θ_{1k}, θ_{2k}, and λ, should be interpreted as the effect of a marginal change in a given variable in *one* of the neighbors.

We estimate (2) by OLS, with standard errors corrected à la Hsiang (2010).

Model III

Part of the observed spatial correlation in conflict is due to the fact that conflict determinants are correlated; part is due to direct contagion. Disentangling these two effects is, in general, difficult. Models allowing for spatial dependence in the dependent variable are known as spatial autoregressive models and are estimated with maximum likelihood or GMM techniques. A further complication arises in our context, since in addition to spatial autocorrelation we expect the process of conflict to be autocorrelated in time. We thus estimate Model III:

section. We are thankful to Nicolas Berman, Mathieu Couttenier, Dominic Rohner, and Mathias Thoenig for sharing the amended version of the code in Hsiang (2010).

$$
\begin{aligned}
&ANY\ EVENT_{c,i,t} = \phi ANY\ EVENT_{c,i,t-1} + \rho W \cdot ANY\ EVENT_{t} + \\
&+ \alpha_c + \sum_{k=0}^{2} \beta_{1k} C_{c,t-k} + \sum_{k=0}^{2} \beta_{2k} GS\_C_{c,t-k} + \mu_{it} + \\
&+ \sum_{k=0}^{2} \theta_{1k} W \cdot C_{t-k} + \sum_{k=0}^{2} \theta_{2k} W \cdot GS\_C_{t-k} + W \cdot \mu_t + \varepsilon_{c,i,t}
\end{aligned} \tag{3}
$$

where μ_{it} denote country $\times$ year fixed effects and α_c cell fixed effects. We also explore different sets of fixed effects and trends. The model in (3) is a dynamic, spatially autoregressive Durbin model that we estimate by maximum likelihood following Parent & LeSage (2012) and Yu, de Jong, and Lee (2008), clustering standard errors by cell. The likelihood is derived in the Online Appendix, Section C.

Drawing inferences on the impact of local climate shocks on conflict, accounting for spatial spillovers, presents challenges comparable to the estimation of peer effects. As discussed in Gibbons, Overman, and Patacchini (2015), disentangling contextual effects (in our case, local weather shocks that are clustered in space) from direct spillovers (in our case, conflict contagion) requires imposing some structure on the spatial dependence in the process. Such structure is embedded in the spatial matrix. Intuitively, the MLE estimator exploits climate shocks occurring beyond 180 km (among the "second-degree neighbors") as a source of variation in conflict incidence in the immediate neighbors (within 180 km). This is similar in spirit to an instrumental variables approach such that shocks occurring among second-degree neighbors instrument for conflict occurring among the immediate neighbors. We discuss an instrumental variable version of our estimates in section 4.1. Our implicit identifying assumption is thus that rainfall beyond 180 km is not affecting conflict in the own cell, other than by inducing more local conflict that then spills over in space. While this is by definition not testable, in section 6.1 we discuss robustness to various distance cutoffs.

The estimation of spatially and temporally autoregressive terms is an innovation of our paper and is particularly relevant when the data are highly disaggregated, and hence highly spatially correlated. Ignoring the term $W \cdot Y$ can lead to omitted variable bias: all of the observed spatial clustering in conflict would be attributed to conflict determinants that happen to be clustered spatially, and the contemporaneous impact of climate shocks would tend to be overestimated.[7] On the other hand, if one included $W \cdot Y$ but estimated the model via OLS, estimates would suffer from simultaneity bias in the opposite direction, overestimating spillover effects and underestimating the local impact of shocks.

3 Data

3.1 Sources and dataset construction

We bring together high-frequency, geo-referenced data from a variety of sources and construct a dataset covering 46 African countries over the period 1997 through 2011. Details on countries and sources can be found in the Online Appendix, section A.

Conflict data

Data on conflict come from the PRIO/ Uppsala ACLED dataset, covering 1997 through 2011. ACLED codes the latitude, longitude, and date of a wide range of conflict-related events, including battles and activities involving rebels, such as recruitment or the establishment of headquarters. Event data are derived from reports from war zones, humanitarian agencies, and research publications. While there may be selection in reporting, it is unclear that such bias would be systematically correlated with our measure of cell-specific growing season weather shocks. We also explore robustness to using the alternative Uppsala Conflict Data Program Georeferenced Event Dataset (UPCDP-GED), which follows a different coding strategy (see Online Appendix, section A).

Climate data

Our main climate indicator is the Standardized Precipitation-Evapotranspiration Index (SPEI), developed by Vicente-Serrano et al. (2010). While most of the conflict literature has focused on precipitation, the impact of rainfall on the growing cycle of a plant depends also on the ability of the soil to retain water. This is captured by "potential evapotranspiration," which in turn depends on temperature, latitude, sunshine exposure, and wind speed. SPEI reflects this and has been found to generally outperform other indexes in predicting crop yields (Vicente-Serrano et al., 2012).

The climate inputs we employ to compute SPEI are drawn from a high-quality re-analysis dataset (ECMWF ERA-Interim), which relies on weather stations, satellites, and sondes. SPEI

[7] An alternative way to frame this is to note that Models I and II are the reduced form version of Model III: the coefficients of climate variables capture the equilibrium effect of local and neighboring shocks, gross of direct conflict spillovers that they may have induced.

is expressed in units of standard deviation from the cell's historical average and thus has mean 0 by construction in the historical sample (1979-2011 in our case). Sections A and B of the Online Appendix include further details on the inputs and computation of SPEI.

Crop calendars and crop-specific climate shocks

Our analysis exploits periods within the year during which climatic conditions affect agricultural production the most. We identify the main crop, by harvested area, cultivated in each cell as of the year 2000, drawing on Monfreda, Ramankutty, and Foley (2008). We then retrieve its cell-specific growing season, based primarily on the MIRCA 2000 crop calendars dataset (Portmann, Siebert, & Döll, 2010). We then match our monthly climate data with the calendars of the crops cultivated in each cell, thus creating cell-specific measures of "relevant" climatic conditions.

Our key climate indicator, denoted as *SPEI Growing Season*, is computed by averaging monthly SPEI over the growing season months of a cell's main crop in a given year. Higher values of this variable correspond to more favorable conditions for local agriculture. For the sensitivity analysis in Table A10, we consider alternative functional forms and widely used indicators such as rainfall and temperature.

Other data

We complement our dataset with a number of cell-level characteristics related to geography, infrastructure, and ethnic fractionalization that we employ as control variables or sources of heterogeneity. These variables are described in the Online Appendix, section A, and summary statistics are reported in Appendix Table A1. Section D in the Appendix also discusses cross-sectional estimates relating cell-level characteristics to conflict propensity.

3.2 Descriptive statistics

Table 1 reports descriptive statistics. The average cell in our sample has experienced conflict episodes for 17 percent of the years, which means 2.5 years. The mean of SPEI in our sample is -0.11, indicating that weather conditions throughout 1997-2011 have been less favorable to agriculture compared to the 1979-2011 historical sample over which SPEI is computed.

In Figure 1 we map our key variables, to get a sense of their within-country variation. Figure 1A shows conflict prevalence, reporting the fraction of years during 1997 through 2011 in which each cell experienced at least one conflict event. Conflict appears to be clustered in space, and in particular in the Great Lakes region and in West Africa. Figure 1B plots average SPEI (for comparison, Appendix Figure A1 plots average rainfall). Although SPEI appears to be spatially correlated, it displays more local variation than rainfall. Appendix Figure A3 maps the distribution of crops, showing that a wide range of crops are cultivated in our sample, which gives us significant variation in climate across cells and months thanks to variation in the growing season of different crops.

4 Empirical results

Our dependent variable is $ANY\ EVENT_t$, a dummy equal to 1 if the cell experienced at least one conflict event during year t. As discussed in section 2.2, we consider three models: a non-spatial, static model (Model I), a non-autoregressive spatial static model (Model II), and a spatial autoregressive dynamic model (Model III). All specifications include the following cell-level controls: elevation, roughness, area, presence of roads, distance to river, shared cell, border, presence of minerals, and ethno-linguistic fractionalization (ELF). Models II and III also include the spatial lags of controls and of the relevant fixed effects (these coefficients are not reported for ease of exposition).

4.1 Benchmark estimates

Table 2 contains our main results. The regressor of interest is *SPEI Growing Season*, defined as the average level of SPEI during the main crop's growing season. Higher values of this variable correspond to higher "effective" rainfall. We also control for standalone SPEI, which in this specification captures the impact of SPEI in months outside the growing season of the main crop. The first and second temporal lag are included for all climate indicators.

Column 1 shows that the contemporaneous effects of SPEI inside and outside the growing season essentially offset one another. However, high values of *SPEI Growing Season* reduce conflict likelihood in the following year and the year after that, whereas lagged SPEI outside of the growing season has no significant impact. When we introduce the spatial lag of our climate variables (column 2), standalone SPEI becomes insignificant also contemporaneously and only the first lag of *SPEI Growing Season* remains negative and significant. This is consistent with the idea that conditions during the growing season are those which matter the most for agriculture. The fact that conflict responds with a one-year lag parallels the temporal persistence highlighted in cross-country studies (e.g., Ciccone, 2013). If this variable affects conflict through rural incomes, it could plausibly take one full agricultural season for these seasonal weather patterns to translate into an economic shock. The coefficients on the spatial lags of the SPEI variables are generally small and do not display a consistent pattern, suggesting that the direct effects of weather shocks are strictly local. We nevertheless include the spatial lags of the regressors in all of our specifications, in order to correctly estimate the coefficient on $W \cdot Y$.

In column 3 we introduce our full spatially and temporally autoregressive model. The coefficient of the first lag of *SPEI Growing Season* in the own cell maintains its negative sign, magnitude, and significance level. A one standard deviation increase in this variable is associated with a 1.5 percentage point reduction in conflict likelihood in the subsequent year, relative to the cell's long-term mean. This is roughly 9 percent of the unconditional mean of the dependent variable.

Conflict spillovers are significant both in time and space. Conflict in a cell in a given year is associated with a 33 percentage point higher probability of conflict the following year. Contemporaneous conflict in one of the neighbors induces a 4 percentage point increase in the probability of conflict in the cell itself. Given that the average cell in our sample has 7.4 neighbors, this means that conflict in *all* of the neighbors induces a 30 percentage point increase in the probability of conflict in the average cell.

As discussed in section 2.2, we estimate Model III by maximum likelihood using spatial econometric techniques. As a validation exercise, in Appendix Table A4 we propose two instrumental variables versions of Model III. In column 4 of Table A4 we instrument for conflict in the immediate neighbors using conflict in the second-order neighbors, an approach similar to those used in time series to address autocorrelation in the dependent variable. In column 7 our instrument is the growing season SPEI of second-order neighbors –an approach similar to that of Bramoullé, Djebbari, and Fortin (2009). In both cases we instrument lagged conflict in the own cell using the second lag of conflict, following the time series literature. Both approaches yield estimates that are comparable, in sign and significance, to those found in Table 2.

Next, we explore robustness to different types of fixed effects. Column 3 includes year fixed effects and a country-specific linear time trend, column 4 includes country × year fixed effects, and column 5 includes cell and country × year fixed effects. The coefficient on *SPEI Growing* $Season_{t-1}$ is remarkably stable in sign and magnitude.

As expected, temporal spillovers are greatly attenuated once we include cell fixed effects, as some of the persistence is attributed to unobserved cell-level long-run characteristics. Nevertheless, relative to a cell's historical conflict propensity, conflict in a given year increases the likelihood of conflict in the subsequent year by 12 percentage points. Spatial spillovers are mildly attenuated once we focus on within-cell conflict variation, possibly because being part of a persistent conflict cluster is one of the time-invariant characteristics picked up by the cell fixed effects. According to column 5 estimates, when a cell experiences conflict each of its neighbors faces a 2.3 percentage point increased conflict likelihood. In the subsequent analysis we adopt the conservative specification of column 5 as our benchmark.

4.2 Impact magnitude and projections

In Model III, the impact of a covariate X on Y in a given cell is not entirely captured by the estimated regression coefficient of that covariate. For instance, the coefficient -0.037 from column 5 of Table 2 should be interpreted as the direct impact of *SPEI Growing Season* on next period's conflict in the own cell. However, a shock in the own cell also affects conflict in neighboring cells, which in turn affect conflict in the own cell through the spatial lag term. As a result, current conflict in the own cell may be amplified. Moreover, the effects of a one-time shock will persist in time, and these impacts will further propagate in space.

To quantify the total effects of a one-time shock we conduct an exercise similar in spirit to the evaluation of an impulse response. We consider Model III and start by setting all explanatory variables and prior conflict to 0; we then provide a hypothetical cell with a one-time negative shock to *SPEI Growing Season* equal to minus one standard deviation; finally, we use the estimates in Table 2, column 5, to track the marginal impact of this shock on the dependent variable in subsequent periods, leaving all other covariates at 0, in the own as well as the neighboring cells. In Figure 2 we report the results of this exercise.

Figure 2a plots the marginal impacts of the one-time decrease in *SPEI Growing Season* on conflict incidence in the five subsequent periods. The solid line refers to the own cell, the dashed to the average neighbor. At $t = 0$ the shock occurs. Conflict in the own cell does not react immediately: the point estimate of the contemporaneous response is slightly negative but insignificant; the neighbor's response is more precisely estimated and is a modest conflict increase, which will feed back in the own cell's response through the term $W \cdot Y$. In the first period after the shock, although no additional shocks occur, conflict in the own cell increases by a total of 1.3 percentage points, close to the point estimate of the first lag of *SPEI Growing Season* (Table 2, column 5) rescaled to the standard deviation of the covariate. After period 3 the marginal effects start fading away. The response of neighbors in Figure 2a roughly mirrors that of the own cell at a much smaller scale, but appears to be more persistent in time.

Figure 2b reports the results of the same exercise, but focusing on space instead of time. For time periods 0, 1, 2, and 4 we map on a grid the marginal impacts of the shock on different cells, representing larger impacts with darker shades. The cell that receives the one-time shock is at the center of the grid and is marked by an x. The definition of neighbors allows only the eight adjacent cells to be directly affected by cell x through their spatial lag terms. However, conflict induced by the one-time shock to cell x does propagate to cells beyond those immediately adjacent, due to spillovers from their own adjacent cells.

The above exercises are also useful to assess the bias from ignoring spillovers. We make this assessment in two ways. First, we have directly compared estimates from Model I with those of Model II and Model III when commenting Table 2. Second, the values in Figure 2a can be compared to the coefficients of Model I. Taken together, these results suggest that neglecting spatial spillovers leads to lower estimated impacts of lagged SPEI on conflict.

While in Figure 2 we employ a one-time, artificial shock, the same method can be used to feed into the process actual projected shocks. We repeat the above procedure feeding into the process forecast values of *SPEI Growing Season* for 2016 through 2050, to get a sense of how climate change will affect conflict likelihood, all else being equal and under the assumption that the responsiveness of conflict to SPEI remains constant in the future.

The first step involves computing projections of future SPEI shocks. We draw on cell-level precipitation and temperature projections obtained from a variety of climate models and under a range of emissions scenarios, all belonging to the World Climate Research Programme's Coupled Model Intercomparison Project phase 5 (CMIP5). Our benchmark model is FGOALS-g2, under a RCP 2.6 emissions scenario - a conservative one that assumes a peak in greenhouse gas emissions between 2010 and 2020 followed by a decline throughout the rest of the 21st century. A description of our sources and forecasting methodology is provided in the Online Appendix, sections A and B. The average of *SPEI Growing Season* (which is -0.025 in our 1997-2011 sample) becomes -0.135 in the 2016-2050 projected sample, indicating that the average cell experiences shortages of rainfall relative to its historic mean. Average projected values of *SPEI Growing Season* over 2016 through 2050 are reported in Figure A4. Next, we obtain for each cell and year the marginal change in conflict incidence induced by *SPEI Growing Season* shocks, according to Model III (Table 2, column 5). This marginal change reflects current and past shocks, among neighbors and in the own cell, due to the mechanisms discussed in Figure 2. Figure A5 maps these marginal changes in each cell, averaged over 2016 through 2050. The pattern clearly overlaps with that in Figure A4.

In an average year, conflict increases by 1.2 percentage points relative to a cell's historic mean (approximately a 7 percent increase) due to SPEI shocks. Note that this reflects averages over cells that experience negative shocks and also cells that experience positive ones. The peak marginal increase in conflict is over 4 percentage points, or about 23 percent of the 1997-2012 average conflict incidence. As a comparison, Burke et al. (2009) predict an increase in conflict incidence between 43% and 56% by 2030, though the larger magnitude may depend on the fact that they include country and not cell fixed effects. In Appendix Table A5 we perform a sensitivity analysis of these results to different climate models and emissions scenarios, as recommended by Burke, Hsiang, and Miguel (2015). Our estimates are remarkably stable. We must however be cautious in taking these estimates literally, as they do not account for crop mix adaptation (Costinot, Donaldson, & Smith, 2016), and we hold constant a number of socioeconomic and political variables that may evolve endogenously over the long run.

5 Mechanisms and heterogeneous effects

Our benchmark estimates indicate that favorable weather during the growing season decreases the likelihood of conflict, while outside the growing season it does not. This is consistent with an "opportunity cost" mechanism related to local agricultural incomes and rules out direct effects through channels such as violence due to extremely hot weather. It also rules out a predation mechanism, by which cells experiencing agricultural booms would be *more* likely to experience conflict. In this section we further explore competing mechanisms using multiple approaches.

5.1 Channels

In Table 3 we examine heterogeneous effects in the impact of cell-level weather conditions. We revisit our benchmark specification (Table 2, column 5), augmenting it with interactions between *SPEI Growing Season* and cell-level characteristics capturing alternative channels. Spatial lags of the SPEI regressors are included in all specifications, but not reported in the table for brevity. The first channel relates to the logistics of warfare: precipitation might affect conflict directly by causing floods and hindering the movement of troops. Given that this should not be systematically correlated with the timing of the growing season, our benchmark estimates do not lend support to this interpretation. However, to further investigate this hypothesis, in column 1 we interact growing season weather with a proxy for road infrastructure in the cell: the presence of at least one road of primary use. The coefficient on the first lag of this interaction is negative and significant at the 10% level. This could indicate that seasonal weather interacts with the logistics of troop movements, but could also reflect the greater strategic importance of locations near a major road.

The second channel relates to state capacity. Fearon & Laitin (2003) argue that civil conflict is more prevalent in countries with poor state capacity, which have limited resources for counterinsurgency or for redistribution. This explanation emphasizes state capacity at the national level, whose fluctuations are captured in our specification by country $\times$ year dummies. Nevertheless, local dimensions of state capacity may be correlated with cell-level weather. In column 2 we interact our weather variables with the tax-to-GDP ratio, drawn from Cagé and Gadenne (2014). The coefficient on the interaction with *SPEI Growing Season*$_{t-1}$ is positive and significant, suggesting that the local effects of weather on conflict are attenuated in countries with better state capacity.

The third mechanism is related to grievances: weather shocks might exacerbate (perceived) inequalities between groups. Democracy and civil liberties should be associated with a lower risk of grievance-induced conflict, as they provide room for requesting redistribution peacefully. In column 3 we interact our weather variables with the Polity IV combined polity score (Marshall, Jaggers, & Gurr), and do not find significant effects.[8] Finally, we turn to ethnic cleavages as a potential source of grievances. In column 4 we consider the number of discriminated groups in a cell as a proxy for latent ethnic conflict. This is drawn from the GeoEPR-ETH dataset (see Online Appendix, section A). We consider groups classified as "subjected to active, intentional, and targeted discrimination, with the intent of excluding them from both regional and national power" at the beginning of our sample. The interaction with the first lag of *SPEI Growing Season* is negative and significant, suggesting that preexisting grievances are more likely to turn into violent conflict following an agricultural shock. We pursue this idea further by considering ethnicities that are partitioned across country borders and that may advance secessionist demands or seek military assistance from coethnics across the border (Michalopoulos

[8]This index, measured at the country-year level, ranges from -10 (strongly autocratic) to $+10$ (strongly democratic).

and Papaioannou, 2016). We construct an indicator for whether a cell contains a border that cuts through an ethnic homeland ("Partition" in column 5) and interact it with *SPEI Growing Season*. Homelands are defined based on the GREG dataset (see Online Appendix, section A). We do not find significant effects, although the interaction with *SPEI Growing Season*$_{t-1}$ has the expected negative sign and is quite large in magnitude.

5.2 Heterogeneous spatial spillovers

In this section we investigate heterogeneous effects in spatial persistence, which can be informative of conflict spillover channels. The literature has proposed a number of mechanisms (see, e.g., Buhaug and Gleditsch, 2008). First, conflict may disrupt the local economy, reducing the opportunity cost of fighting in neighboring areas. It may also induce an inflow of arms or attract mercenaries who move across the territory. Finally, rebellion may induce emulation. Additional mechanisms are specific to cross-country spillovers (e.g. Gleditsch, 2007). Refugee flows across countries may induce tensions leading to conflict; arms trading may be particularly pronounced near the border; irredentist demands may involve territory across two nations.

To shed light on the pass-through of conflict across cells, we vary the definition of what constitutes a neighbor and estimate specifications analogous to our benchmark but differing in the spatial weighting matrix used to define $W \cdot Y$. The results are reported in Table 4. Each column reports the coefficient on $W \cdot Y$ from a different regression, with the column header indicating how W is defined in that specification.[9]

In columns 1 and 2 we investigate whether spillovers are stronger across national borders. We consider two sets of neighbors: adjacent cells that belong (column 1) or not (column 2) to the same country. We detect positive spillovers in both cases, stronger when considering neighbors from a different country.

We next examine spillovers across ethnicities and country boundaries.[10] Coethnics residing across the border can provide rebels with resources and protection (Bosker and de Ree, 2014). Columns 3 and 4 consider the role of coethnics alone: we consider as neighbors adjacent cells that share (column 3) or do not share (column 4) the same main group.[11] The size of the spillover effect is comparable across the two sets of neighbors. Interesting differences emerge,

[9] We continue to employ our benchmark weighting matrix when defining spatial lags in the covariates, so as to make the specifications comparable across columns.

[10] For a network analysis of rebel behavior that incorporates rainfall patterns in ethnic homelands, see König et al. (2017).

[11] We rank ethnic groups based on their share of the territory according to the GREG dataset.

however, when we consider the interaction of ethnicity and borders. Within the same country, spillovers are not differential across ethnic homelands (column 5 versus column 6); cross-country spillovers are instead more pronounced across ethnic boundaries (column 7 versus column 8). These findings could reflect differences in the nature of conflicts occurring in the interior of a country versus in bordering areas. For example, conflicts occurring near boundaries may be separatist in nature and may spill over to areas occupied by different ethnic groups. They may also be more likely to generate refugee flows that fuel interethnic tensions. On the other hand, conflicts occurring in the interior are likely to have (non-separatist) objectives and follow a different diffusion process. Besides direct conflict spillovers, our data present an additional source of spatial dependence: spatial decay in the effects of agricultural shocks . The coefficients of the spatial lags of *SPEI Growing Season* are generally small, indicating that the direct effects of local shocks dissipate rapidly in space. However, this could also result from heterogeneous effects across neighbors operating in opposite directions. We explore this in the Appendix, section E. Appendix Table A6 shows that only shocks occurring among coethnic neighbors and among neighbors cultivating the same main crop increase conflict in the own cell. This provides suggestive evidence that coinsurance within the ethnic group may not be effective in the presence of uniform crop patterns across space.

5.3 Different types of conflict events

We next turn to a disaggregation of conflict events into four types, based on the ACLED classification. The dummy BATTLE equals 1 when a cell/year has experienced a battle of any kind, regardless of whether control of the contested location changes. The dummy CIVILIAN captures violence against civilians, defined in ACLED as instances where "any armed group attacks unarmed civilians within a larger conflict." This is the type of event most closely related to possible predation motives. Riots and protests (dummy RIOT) are instances in which "a group is involved in a public meeting against a government institution." ACLED also codes non-violent rebel activities, such as the establishment of a base or headquarters and recruitment drives.[12] These are particularly interesting to test theories that stress the opportunity cost of fighting, and we aggregate them in the binary variable REBEL. Summary statistics in Table 1 indicate that the average frequency of these events in the cell/years in our sample is .10 for

[12]In the ACLED codebook, these correspond to events of type 4 ("headquarters or base established") or 5 ("non-violent activity," which includes recruitment drives, incursions, and rallies).

battles, .10 for violence against civilians, .06 for riots, and .03 for rebel recruitment.

In Table 5 we examine the effects of climate on different types of events.[13] The coefficients of the temporal autoregressive terms are in the $0.07 - 0.14$ range. Battles and rebel recruitment have the highest degree of temporal persistence, whereas riots appear less persistent in time, possibly due to the intermittent nature of these episodes. The coefficients on the spatial autoregressive terms range from 0.004 for riots to 0.02 for battles and violence against civilians, suggesting that more violent episodes are more likely to spill over in space. The coefficients on own climate shocks point in the same direction as in the aggregate results, with the first lag of *SPEI Growing Season* associated with lower incidence of conflict events (albeit insignificant for riots). The effect sizes are largest for rebel recruitment, followed by violence against civilians: for a one standard deviation shock to *SPEI Growing Season*, the standardized point estimates are 24 percent and 17 percent of the mean of the dependent variable. This points toward theories based on the opportunity cost of rebel recruitment.

5.4 Different conflict actors

We next exploit the breakdown of conflict by type of actor. For each event, ACLED reports the identity of the perpetrator and the victim and classifies them as government, rebel force, or civilians. By investigating which actors initiate conflict or are attacked following a SPEI shock, we can shed more light on mechanisms. We focus on three sets of actors: the government, politically violent actors (rebels, political militias, ethnic militias), and non-organized actors (a category in which we pool civilians, rioters, and protesters).[14]

About 32 percent of the events are initiated by the government, 21 percent by rebels, and 27 percent by political militias. Rioters, protesters, and civilians are the most common victims (38 percent of events), followed by rebels (23 percent). We start by disaggregating our dependent variable by perpetrator-victim pairs. For example, we can construct a dummy equal to 1 if a cell experienced at least one event involving the government as perpetrator and a rebel force as victim. For each actor-pair we estimate our benchmark specification (Table 2, column 5) and focus on the coefficient of *SPEI Growing Season*$_{t-1}$. We report these coefficients in Table 6. Each cell in the matrix shows the coefficient from a different regression, corresponding to

[13] The Appendix also reports cross-sectional estimates for the impact of cell-level geographic covariates on different types of conflict events (section D and Table A3).

[14] As per ACLED, rebel groups are violent actors with a stated political agenda for national power. Political militias are actors with a political purpose who do not seek the removal of a national power. Ethnic militias are violent groups who claim to operate on behalf of a larger identity community (Raleigh & Dowd, 2016).

a different perpetrator-victim pair. Rows correspond to perpetrators and columns to victims. A number of interesting patterns arise. The main perpetrators of attacks induced by SPEI shocks are political militias and rioters attacking mostly the government and rebel forces. This supports the opportunity cost interpretation, but is also compatible with a state capacity effect. Rioters, protesters, and civilians are also victimized, consistent with our finding that SPEI shocks lead to violence against civilians. Of the non-government victims, ethnic and political militias seem unaffected by SPEI shocks, possibly because their recruiting strategies may be more identity-based.

5.5 Conflict onset and termination

Our analysis so far has focused on conflict incidence. We now briefly discuss the results for conflict onset and termination, which we report in Appendix Table A7. Conflict onset is a binary indicator that takes value 0 in years of peace and 1 in the first year in which a cell experiences conflict, and is missing in subsequent conflict years. Conflict termination equals 0 in years of conflict and 1 in the first year with no conflict after a spell of conflict, and is missing in subsequent peace years.[15] In Table A7 we present estimates of Model II for onset and termination. As explained in section 2.2, we cannot estimate Model III with these dependent variables because the estimation of autoregressive Durbin models requires a balanced panel. Table A7 should thus be taken cautiously, as Model II does not account for direct conflict spillovers.

Our explanatory variable of interest, *SPEI Growing Season*$_{t-1}$, is significantly correlated with the onset of conflict broadly defined (column 1) and especially the onset of battles (column 2), violence against civilians (column 3), and non-violent rebel activities (column 5). Relative to the mean of the dependent variable, the impacts are largest for rebel activities, followed by violence against civilians, mirroring our findings for conflict incidence. This suggests that agriculture-relevant shocks might be especially important as local triggers of new conflict spells, particularly through the opportunity cost channel. The effect is negative but insignificant for conflict termination (column 6).

[15] Since the majority of cell/years in the sample experiences no conflict events, conflict termination is non-missing in a very small sample. This prevents us from disaggregating by type of event when analyzing conflict termination.

6 Robustness

In this section we explore the sensitivity of our estimates to different grid resolutions, different choices of spatial weighting matrix, and alternative climate indicators.

6.1 Sensitivity to spatial resolution and distance

Just as in time series the structure of temporal dependence is assumed by the researcher and is not estimated, so is the structure of spatial dependence implied by the choice of grid resolution and spatial weighting matrix. In Appendix Table A8 we present our benchmark specification (Table 2, column 5) estimated on gridded datasets of different spatial scales.[16] In column 1 we consider a higher-resolution $0.5\times$ 0.5-degree grid, placed in such a way that four 0.5-degree cells are contained in one of our benchmark 1-degree cells. In columns 2 to 5 we consider a lower-resolution $2\times$ 2 grid, obtained aggregating four of our 1×1 original cells in a single "macro-cell." This coarser grid can be constructed in four different ways, depending on where such "macro-cells" are centered; hence we report estimates obtained with each of these four grids.[17] The 1-degree grid we used throughout the paper appears to provide more precise estimates than those obtained with higher or lower resolutions, validating our choice. The effects of SPEI may not be captured at very high resolutions because a drought in a limited area may not have enough of an impact on local incomes when there is smoothing across agricultural markets; at the same time, the effects may be washed out at lower resolutions because fixed effects at the macro-cell level may absorb too much of the variation.

In Appendix Table A9 we turn to the choice of spatial weighting matrix. The latter is particularly relevant as the exclusion restriction on which our MLE estimates are based is that shocks occurring in second-order neighbors do not directly affect conflict in the own cell. The most popular choices in the literature are binary contiguity matrices, that we consider in columns 1 to 3, and matrices based on the inverse geographic distance, which we examine in columns 4 to 6. In columns 1 to 3 we estimate our model using binary contiguity matrices with different distance cutoffs: 290, 450 and 600 km.[18] When we increase the radius of our

[16]This exercise addresses the Modifiable Areal Unit Problem (MAUP) that commonly arises with spatial data (Heywood, Cornelius, & Carver, 1998).

[17]When estimating our specification for the 0.5- and the 2-degree grids, we employ binary contiguity matrices with cutoffs of 90 and 390 km respectively, so that each cell's neighborhood is formed by the eight adjacent cells at both resolutions.

[18]With distance cutoffs of 290, 450, and 600 km the average number of neighbors for each cell is respectively 18, 44, and 81.

distance matrix, the coefficient on *SPEI Growing Season*$_{t-1}$ becomes increasingly smaller and eventually loses significance. The temporal autoregressive coefficient is very stable around the value of .12 and is significant at the 1 percent level in all specifications. On the other hand, as expected, the choice of weighting matrix does affect the spatial autoregressive coefficient (the coefficient on $W \cdot Y$), which decreases in magnitude as we increase the distance cutoff. This is intuitive: as we add neighbors farther away from the cell, the impact of the average neighbor is driven down. These patterns are confirmed in columns 4, 5, and 7, in which we employ an inverse distance-based weighting matrix.

6.2 Other climate indicators

In Appendix Table A10 we turn to other potential climate indicators and functional forms, including stand-alone SPEI averaged over the entire year (column 1), a measure of drought spells (column 2), nonlinear effects of *SPEI Growing Season* (column 3), and an extended version of this variable that includes the three main crops instead of just the main one (column 4). Details are provided in the Online Appendix, section E. Results obtained with SPEI-based indicators are qualitatively consistent with our benchmark, although only the first lag of our main variable of interest remains significant in column 3. The coefficients on plain measures of rainfall and temperature, averaged over the growing season, have the expected signs but are mostly insignificant.

The contrast with the existing literature, which finds significant effects of rainfall and temperature, may be rationalized by observing that our specification with both spatial and temporal lags of the dependent variable absorbs a lot of the variation in conflict, which is already reduced by the inclusion of cell fixed effects. The richness of SPEI, which embeds information on precipitation and temperature but also on latitude, month of the year, number of sunlight hours, etc., allows us to obtain more precise estimates when we use our benchmark variable.

6.3 Alternative data sources and specifications

In Appendix Table A11 we explore robustness to the choice of conflict dataset by reestimating Table 2 employing the UPCDP-GED dataset, described in the Online Appendix, section A. The qualitative patterns are similar to those obtained with ACLED, although the coefficient on *SPEI Growing Season*$_{t-1}$ becomes smaller and insignificant as we add autoregressive terms, arguably because GED data features less variation in the dependent variable.[19] In terms of magnitudes, according to Model III estimates in columns 3 to 5, the impact of a one standard deviation increase in *SPEI Growing Season* reduces GED-based conflict incidence in the following year by 5% to 7% of the mean of the dependent variable, in line with our ACLED-based estimates.

In Appendix Table A12 we consider different temporal lag structures and find that the significance of the first lag is consistent across specifications. As a placebo, in column 3 we also include a specification with four lags and four leads in *SPEI Growing Season.* Reassuringly, we find leads not to be significant conflict predictors.

7 Conclusions

In this paper we conduct a spatially disaggregated analysis of the determinants of conflict in Africa over the period 1997 through 2011. We exploit within-year variation in the timing of weather shocks and in the growing season of different crops, as well as spatial variation in crop cover, to construct an original measure of weather that is relevant for agricultural production. We find that improved weather during the growing season of the main crops cultivated in the cell significantly reduces conflict incidence. We use state-of-the-art spatial econometric techniques to test for the presence of temporal and spatial spillovers in conflict, and we find both to be sizable and highly significant. These results indicate that caution should be exercised when interpreting results of studies that do not incorporate spatial dynamics. Finally, we use our estimates to predict potential future conflict scenarios induced by climate change, under the assumption that the responsiveness of conflict to weather shocks remains constant in the next decades. Using a variety of models and emissions scenarios, we predict that shocks occurring during the growing season, as per the definition of our main explanatory variable, should become 5.4 times more pronounced during the next 35 years. This in turn leads to an increase in average conflict incidence of 7 percent.

Our findings indicate that the correlates of civil conflict have a strong local dimension and that the likelihood of conflict is not constant in time or in space, even within the same country. This suggests that policy interventions, be they in the form of monitoring, prevention, or peace-keeping efforts, should be targeted in space and time. Our results may be especially relevant when assessing appropriate policy responses to global warming scenarios. Given the link we

[19] Another potential explanation is that GED records only events involving casualties, within conflicts that involve at least 25 battle-related deaths per year, whereas ACLED also codes low-intensity conflict episodes.

trace between shocks affecting agricultural yields and conflict risk, policies aimed at mitigating the effects of climate change on agriculture may be particularly desirable. These include the development of drought-resistant crop varieties, investments in irrigation, and schemes to improve soil water retention. On the other hand, complementary measures to reduce the adverse impacts on incomes, such as weather-indexed crop insurance, also constitute a valuable policy option. Finally, given the increasing availability of high-resolution data (e.g., gridded datasets) and the growing number of research contributions that employ these data to address important development questions, we hope our study can provide a number of insights and methodological indications that are useful for future work.

References

[1] Almer, Christian, Jérémy Laurent-Lucchetti, and Manuel Oechslin, "Water Scarcity and Rioting: Disaggregated Evidence from Sub-Saharan Africa," *Journal of Environmental Economics and Management* 86 (2017), 193-209.

[2] Anselin, Luc, *Spatial Econometrics: Methods and Models*, Boston: Kluwer Academic, (1988).

[3] Bazzi, Samuel, and Christopher Blattman, "Economic Shocks and Conflict: Evidence from Commodity Prices," *American Economic Journal: Macroeconomics* 6:4 (2014), 1-38.

[4] Berman, Nicolas, and Mathieu Couttenier, "External Shocks, Internal Shots: The Geography of Civil Conflicts," *Review of Economics and Statistics* 97:4 (2015), 758-776.

[5] Berman, Nicolas, Mathieu Couttenier, Dominic Rohner, and Mathias Thoenig, "This Mine Is Mine! How Minerals Fuel Conflicts in Africa," *American Economic Review* 107:6 (2017), 1564-1610.

[6] Blattman, Christopher, and Edward Miguel, "Civil War and the Study of Economics," *Journal of Economic Literature* 48:1 (2010), 3-57.

[7] Bosker, Maarten, and Joppe de Ree, "Ethnicity and the Spread of Civil War," *Journal of Development Economics* 108 (2014), 206-221.

[8] Bramoullé, Yann, Habiba Djebbari, and Bernard Fortin, "Identification of Peer Effects through Social Networks," *Journal of Econometrics* 150 (2009), 41-55.

[9] Brückner, Markus, and Antonio Ciccone, "Rain and the Democratic Window of Opportunity," *Econometrica* 79:3 (2011), 923-947.

[10] Buhaug, Halvard, "Climate Not to Blame for African Civil Wars," *Proceedings of the National Academy of Sciences of the USA* 107:38 (2010), 16477-16482.

[11] Buhaug, Halvard, and Kristian Skrede Gleditsch, "Contagion or Confusion? Why Conflicts Cluster in Space," *International Studies Quarterly* 52:2 (2008), 215-233.

[12] Burgess, Robin, Olivier Deschenes, Dave Donaldson, and Michael Greenstone, "Weather and Death in India," working paper (2013).

[13] Burke, Marshall, John Dykema, David B. Lobell, Edward Miguel, and Shanker Satyanath, "Incorporating Climate Uncertainty into Estimates of Climate Change Impacts, with Applications to U.S and African Agriculture" *Review of Economics and Statistics* 97:2 (2015), 461-471.

[14] Burke, Marshall B., Edward Miguel, Shanker Satyanath, John A. Dykema, and David B. Lobell, "Warming Increases the Risk of Civil War in Africa," *Proceedings of the National Academy of Sciences of the USA* 106:37 (2009), 20670-20674.

[15] Burke, Marshall, Solomon M. Hsiang, and Edward Miguel, "Climate and Conflict," *Annual Review of Economics* 7 (2015), 577-617.

[16] Cagé, Julia, and Lucie Gadenne, "Tax Revenues, Development, and the Fiscal Cost of Trade Liberalization, 1792-2006," working paper, (2014).

[17] Ciccone, Antonio, "Estimating the Effect of Transitory Economic Shocks on Civil Conflict," *Review of Economics and Institutions* 4:2 (2013), 1-14.

[18] Collier, Paul, and Anke Hoeffler, "On the Economic Causes of Civil War," *Oxford Economic Papers* 50 (1998), 563-573.

[19] Conley, Timothy G., "GMM Estimation with Cross-sectional Dependence," *Journal of Econometrics* 92:1 (1999), 1-45.

[20] Costinot, Arnaud, Dave Donaldson, and Cory B. Smith, "Evolving Comparative Advantage and the Impact of Climate Change on Agricultural Markets: Evidence from 1.7 million Fields Around the World," *Journal of Political Economy* 124 (2016), 205-248.

[21] Couttenier, Mathieu, and Raphael Soubeyran, "Drought and Civil War In Sub-Saharan Africa," *The Economic Journal* 124:575 (2014), 201-244.

[22] Dal Bó, Ernesto, and Pedro Dal Bó, "Workers, Warriors, and Criminals: Social Conflict in General Equilibrium," *Journal of the European Economic Association* 9:4 (2011), 646-77.

[23] Dell, Melissa, "Path Dependence in Development: Evidence from the Mexican Revolution," working paper, (2012).

[24] Dell, Melissa, Benjamin F. Jones, and Benjamin A. Olken, "Temperature Shocks and Economic Growth: Evidence from the Last Half Century," *American Economic Journal: Macroeconomics* 4:3 (2012), 66-95.

[25] Fearon, James D., and David D. Laitin, "Ethnicity, Insurgency, and Civil War," *American Political Science Review* 97:1 (2003), 75-90.

[26] Gibbons, Steve, Henry G. Overman, and Eleonora Patacchini, "Spatial Methods" (pp. 115-168), in Gilles Duranton, J. Vernon Henderson and William Strange, eds., *Handbook of Regional and Urban Economics*, volume 5a (Amsterdam: Elsevier, 2015).

[27] Gleditsch, Kristian Skrede, "Transnational Dimensions of Civil War," *Journal of Peace Research* 44:3 (2007), 293-309.

[28] Heywood, Ian, Sarah Cornelius, and Steve Carver, *Introduction to Geographical Information Systems* (New York: Addison Wesley Longman, 1998).

[29] Hsiang, Solomon M., "Temperatures and Cyclones Strongly Associated with Economic Production in the Caribbean and Central America," *Proceedings of the National Academy of Sciences of the USA* 107 (2010), 15367-15372.

[30] Hsiang, Solomon M., Marshall Burke, and Edward Miguel, "Quantifying the Influence of Climate on Human Conflict," *Science* 341:6151 (2013).

[31] Hsiang, Solomon M., Kyle C. Meng, and Mark A. Cane, "Civil Conflicts are Associated with the Global Climate," *Nature* 476 (2011), 438-441.

[32] Jia, Ruixue, "Weather Shocks, Sweet Potatoes and Peasant Revolts in Historical China," *The Economic Journal* 124:575 (2014), 92-118.

[33] König, Michael D., Dominic Rohner, Mathias Thoenig, and Fabrizio Zilibotti, "Networks in Conflict: Theory and Evidence from the Great War of Africa," *Econometrica* 85:4 (2017), 1093-1132.

[34] Kudamatsu, Masayuki, Torsten Persson, and David Strömberg, "Weather and Infant Mortality in Africa," working paper, (2017).

[35] Maccini, Sharon, and Dean Yang, "Under the Weather: Health, Schooling, and Socioeconomic Consequences of Early-life Rainfall," *American Economic Review* 99:3 (2009), 1006-1026.

[36] Madestam, Andreas, Daniel Shoag, Stan Veuger, and David Yanagizawa-Drott, "Do Political Protests Matter? Evidence from the Tea Party Movement," *Quarterly Journal of Economics* 128:4 (2013), 1633-1685.

[37] Marshall, Monty G., Keith Jaggers, and Ted Robert Gurr, "Polity IV Project, Political Regime Characteristics and Transitions, 1800-2013," Center for Systemic Peace.

[38] Michalopoulos, Stelios, and Elias Papaioannou, "The Long-Run Effects of the Scramble for Africa," *American Economic Review* 106:7 (2016), 1802-1848.

[39] Miguel, Edward, Shanker Satyanath, and Ernest Sergenti, "Economic Shocks and Civil Conflict: An Instrumental Variables Approach," *Journal of Political Economy* 112 (2004), 725-753.

[40] Monfreda, Chad, Navin Ramankutty, and Jonathan A. Foley, "Farming the Planet: Geographic Distribution of Crop Areas, Yields, Physiological Types, and Net Primary Production in the Year 2000," *Global Biogeochemical Cycles* 22 (2008), 1-19.

[41] O'Loughlin, John, Frank D. W. Witmer, Andrew M. Linke, Arlene Laing, Andrew Gettelman, and Jimy Dudhiab, "Climate Variability and Conflict Risk in East Africa, 1990-2009," *Proceedings of the National Academy of Sciences of the USA* 109:45 (2012), 18344-18349.

[42] Parent, Olivier and James P. LeSage, "Spatial Dynamic Panel Data Models with Random Effects," *Regional Science and Urban Economics* 42:4 (2012), 727-738.

[43] Portmann, Felix T., Stefan Siebert, and Petra Döll, "MIRCA2000 - Global Monthly Irrigated and Rainfed Crop Areas around the Year 2000: A New High-resolution Data Set for Agricultural and Hydrological Modeling," *Global Biogeochemical Cycles* 24:1 (2010), doi:10.1029/2008GB003435.

[44] Raleigh, Clionadh and Caitriona Dowd, "Armed Conflict Location and Event Data Project (ACLED) Codebook," (2015).

[45] Vanden Eynde, Oliver, "Targets of Violence: Evidence from India's Naxalite Conflict," *The Economic Journal* (2017), doi:10.1111/ecoj.12438.

[46] Vicente-Serrano Sergio M., Santiago Beguería, J. Ignacio López-Moreno, Marta Angulo, and Ahmed M. El Kenawy, "A Global 0.5 Gridded Dataset (1901-2006) of a Multiscalar Drought Index Considering the Joint Effects of Precipitation and Temperature," *Journal of Hydrometeorology* 11:4 (2010), 1033-1043.

[47] Vicente-Serrano, Sergio M., Santiago Beguería, Jorge Lorenzo-Lacruz, Jesús Julio Camarero, Juan I. López-Moreno, Cesar Azorin-Molina, Jesús Revuelto, Enrique Morán-Tejeda, and Arturo Sanchez-Lorenzo, "Performance of Drought Indices for Ecological, Agricultural, and Hydrological Applications," *Earth Interactions* 16:10 (2012), 1-27.

[48] Yu, Jihai, Robert de Jong, and Lung-fei Lee, "Quasi-maximum Likelihood Estimators for Spatial Dynamic Panel Data with Fixed Effects when Both N and T are large," *Journal of Econometrics* 146 (2008), 118-134.

Table 1: Summary Statistics

	No. Obs.	Mean	Std. Dev.
ANY EVENT	35042	0.170	0.376
BATTLE	35042	0.097	0.295
CIVILIAN	35042	0.099	0.299
RIOT	35042	0.056	0.231
REBEL	35042	0.030	0.170
SPEI	35042	-0.114	0.571
SPEI Growing Season	35042	-0.025	0.365

Notes: Each observation is a cell/year.

Table 2: Conflict incidence and climate, panel

Dependent variable (Y)=1 if conflict event in year t (ANY EVENT)

	(1)	(2)	(3)	(4)	(5)
	Model I	Model II	Model III	Model III	Model III
	OLS	OLS	MLE	MLE	MLE
Y_{t-1}			0.333***	0.342***	0.121***
			(0.00759)	(0.00769)	(0.00849)
W·Y			0.0449***	0.0291***	0.0229***
			(0.00116)	(0.00127)	(0.00150)
SPEI	0.0334***	0.0150	0.00458	0.00216	-0.00491
	(0.00690)	(0.0144)	(0.0127)	(0.0131)	(0.0132)
SPEI, $_{t-1}$	0.00112	0.0199	0.0107	0.0252*	0.0148
	(0.00698)	(0.0141)	(0.0136)	(0.0142)	(0.0130)
SPEI, $_{t-2}$	0.00883	0.00659	-0.00190	-0.00990	-0.0145
	(0.00701)	(0.0151)	(0.0132)	(0.0138)	(0.0126)
SPEI Growing Season	-0.0329***	-0.00217	0.00122	0.00430	0.0207
	(0.0121)	(0.0149)	(0.0135)	(0.0136)	(0.0129)
SPEI Growing Season, $_{t-1}$	-0.0300**	-0.0399***	-0.0400***	-0.0498***	-0.0367***
	(0.0118)	(0.0148)	(0.0153)	(0.0152)	(0.0139)
SPEI Growing Season, $_{t-2}$	-0.0335***	-0.0238	-0.0145	-0.00523	-0.00925
	(0.0121)	(0.0156)	(0.0144)	(0.0146)	(0.0140)
W·SPEI		0.00379	0.00187	0.00202	5.88e-06
		(0.00234)	(0.00194)	(0.00222)	(0.00220)
W·SPEI, $_{t-1}$		-0.00287	-0.00235	-0.00376	-0.00451**
		(0.00230)	(0.00210)	(0.00239)	(0.00219)
W·SPEI, $_{t-2}$		0.00101	0.00139	0.00453**	0.00329
			(0.00201)	(0.00228)	(0.00211)
W·SPEI Growing Season			-0.00284	-0.00427*	-0.00420*
			(0.00226)	(0.00252)	(0.00248)
W·SPEI Growing Season, $_{t-1}$			0.00464*	0.00621**	0.00648**
		(0.00279)	(0.00250)	(0.00267)	(0.00257)
W·SPEI Growing Season, $_{t-2}$		-0.00260	5.54e-05	-0.00167	0.000522
		(0.00288)	(0.00234)	(0.00261)	(0.00260)
Observations	35,042	35,042	35,042	35,042	35,042
Controls	X	X	X	X	
Year FE	X	X	X		
Country-specific time trend	X	X	X		
Country x Year FE				X	X
Cell FE					X

Notes: Each observation is a cell/year. Standard errors in parenthesis. Columns 1 and 2 corrected for spatial and serial correlation following Hsiang (2010). Columns 3 through 5 corrected for clustering at the cell level. *** p<0.01, ** p<0.05, * p<0.1. W = binary contiguity matrix, cutoff 180 km.

Table 3: Channels of Impact

Dependent variable (Y)=1 if conflict event in year t (ANY EVENT)

	(1)	(2)	(3)	(4)	(5)
Variable Z is:	Roads	Tax to GDP ratio	Polity Score	Number of Discriminated Groups	Partition
Y_{t-1}	0.121***	0.0209	0.121***	0.121***	0.121***
	(0.00850)	(0.0192)	(0.00848)	(0.00849)	(0.00849)
$W \cdot Y$	0.0228***	0.0108***	0.0228***	0.0227***	0.0227***
	(0.00150)	(0.00349)	(0.00150)	(0.00151)	(0.00150)
SPEI Growing Season	0.0150	0.0774	0.0202	0.0239*	0.0197
	(0.0137)	(0.0612)	(0.0128)	(0.0135)	(0.0129)
SPEI Growing Season, $_{t-1}$	-0.0264*	-0.176***	-0.0372***	-0.0297**	-0.0339**
	(0.0149)	(0.0634)	(0.0138)	(0.0146)	(0.0140)
SPEI Growing Season, $_{t-2}$	-0.0165	-0.0357	-0.00942	-0.0102	-0.0117
	(0.0151)	(0.0704)	(0.0140)	(0.0143)	(0.0140)
SPEI Growing Season × *Z*	0.0133	-0.00258	-0.00141	-0.00431	0.00902
	(0.0135)	(0.00349)	(0.00196)	(0.00526)	(0.0174)
SPEI Growing Season, $_{t-1}$ × *Z*	-0.0244*	0.00906**	-0.000115	-0.00943**	-0.0254
	(0.0133)	(0.00371)	(0.00213)	(0.00448)	(0.0167)
SPEI Growing Season, $_{t-2}$ × *Z*	0.0180	0.00269	-0.00119	0.00175	0.0141
	(0.0141)	(0.00420)	(0.00210)	(0.00540)	(0.0165)
Observations	35,042	6,822	35,042	35,042	35,042
W· SPEI variables	X	X	X	X	X
Country x Year FE	X	X	X	X	X
Cell FE	X	X	X	X	X

Notes: Each observation is a cell/year. Estimation by MLE. Standard errors in parenthesis corrected for clustering at the cell level. *** p<0.01, ** p<0.05, * p<0.1. W = binary contiguity matrix, cutoff 180 km.

Table 4: Heterogeneous Conflict Spillovers, Panel

Dependent variable (Y)=1 if conflict event in year t (ANY EVENT)

	(1)	(2)	(3)	(4)	(5)	(6)	(7)	(8)
					Same country		Different country	
Neighbors included in W	Same Country	Different Country	Same Main Group	Different Main Group	Same Main Group	Different Main Group	Same Main Group	Different Main Group
W·Y	0.0217***	0.0308***	0.0222***	0.0248***	0.0217***	0.0219***	0.0275***	0.0340***
	(0.00168)	(0.00372)	(0.00186)	(0.00281)	(0.00199)	(0.00339)	(0.00561)	(0.00475)
Observations	35,042	35,042	35,042	35,042	35,042	35,042	35,042	35,042
Country x Year FE	X	X	X	X	X	X	X	X
Cell FE	X	X	X	X	X	X	X	X

Notes: Each observation is a cell/year. Estimation by MLE. Standard errors in parenthesis corrected for clustering at the cell level. *** $p<0.01$, ** $p<0.05$, * $p<0.1$.

Table 5: Different Types of Conflict Events, Panel

Dependent variable:	*Battle*	*Civilian*	*Riot*	*Rebel*
	(1)	(2)	(3)	(4)
Y_{t-1}	0.131***	0.109***	0.0705***	0.138***
	(0.0106)	(0.0101)	(0.0119)	(0.0165)
$W \cdot Y$	0.0233***	0.0236***	0.00438**	0.0104***
	(0.00174)	(0.00177)	(0.00200)	(0.00230)
SPEI	0.00620	-0.0190*	-0.00502	-0.0133**
	(0.0108)	(0.0109)	(0.00876)	(0.00672)
SPEI, $_{t-1}$	-0.000270	0.0134	0.0180*	0.0127*
	(0.0107)	(0.0106)	(0.00927)	(0.00707)
SPEI, $_{t-2}$	0.00154	-0.000397	-0.0149	-0.0107
	(0.0103)	(0.0101)	(0.00930)	(0.00653)
SPEI Growing Season	0.0133	0.0230**	0.0180**	0.0108
	(0.0109)	(0.0113)	(0.00903)	(0.00738)
SPEI Growing Season, $_{t-1}$	-0.0289**	-0.0454***	-0.0148	-0.0193**
	(0.0116)	(0.0120)	(0.00972)	(0.00783)
SPEI Growing Season, $_{t-2}$	-0.0203*	-0.00800	0.0198**	0.00979
	(0.0122)	(0.0109)	(0.00928)	(0.00764)
W·SPEI	-0.00227	0.00292	0.000648	0.00156
	(0.00179)	(0.00179)	(0.00139)	(0.00108)
W·SPEI, $_{t-1}$	-0.00211	-0.00334*	-0.00169	-0.00216*
	(0.00187)	(0.00174)	(0.00150)	(0.00113)
W·SPEI, $_{t-2}$	-0.000699	0.000674	0.00319**	0.00177*
	(0.00181)	(0.00171)	(0.00146)	(0.00107)
W·SPEI Growing Season			-0.000539	-0.000973
			(0.00152)	(0.00130)
W·SPEI Growing Season, $_{t-1}$			0.00127	0.00252*
			(0.00166)	(0.00138)
W·SPEI Growing Season, $_{t-2}$	0.00446**	0.00171	-0.00444***	-0.00249*
	(0.00224)	(0.00199)	(0.00159)	(0.00135)
Observations	35,042	35,042	35,042	35,042
Country x Year FE	X	X	X	X
Cell FE	X	X	X	X

Notes: Each observation is a cell/year. Estimation by MLE. Standard errors in parenthesis corrected for clustering at the cell level. *** p<0.01, ** p<0.05, * p<0.1. W = binary contiguity matrix, cutoff 180 km.

Table 6: Perpetrators and Victims, Panel

Dependent variable (Y)=1 if conflict event in year t (ANY EVENT)

		Coefficients of SPEI Growing Season, $_{t-1}$				
		ACTOR 2 (Victim)				
		Government	Rebel force	Political militia	Ethnic militia	Rioters, protesters, and civilians
ACTOR 1 (Perpetrator)	Government	-0.0185**	-0.0221**	-0.00625	-0.00428	-0.0267***
	Rebel force	-0.0102	-0.0134*	-0.00365	-0.00276	-0.0144**
	Political militia	-0.0274***	-0.0259***	-0.00626	-0.00352	-0.0300***
	Ethnic militia	-0.0127**	-0.00456	-0.00600	-0.00634	-0.00914
	Rioters, protesters, and civilians	-0.0236***	-0.0127*	-0.0127*	-0.00246	-0.0175**

Notes: Each observation is a cell/year. Estimation by MLE. Standard errors in parenthesis corrected for clustering at the cell level. *** p<0.01, ** p<0.05, * p<0.1. W = binary contiguity matrix, cutoff 180 km.

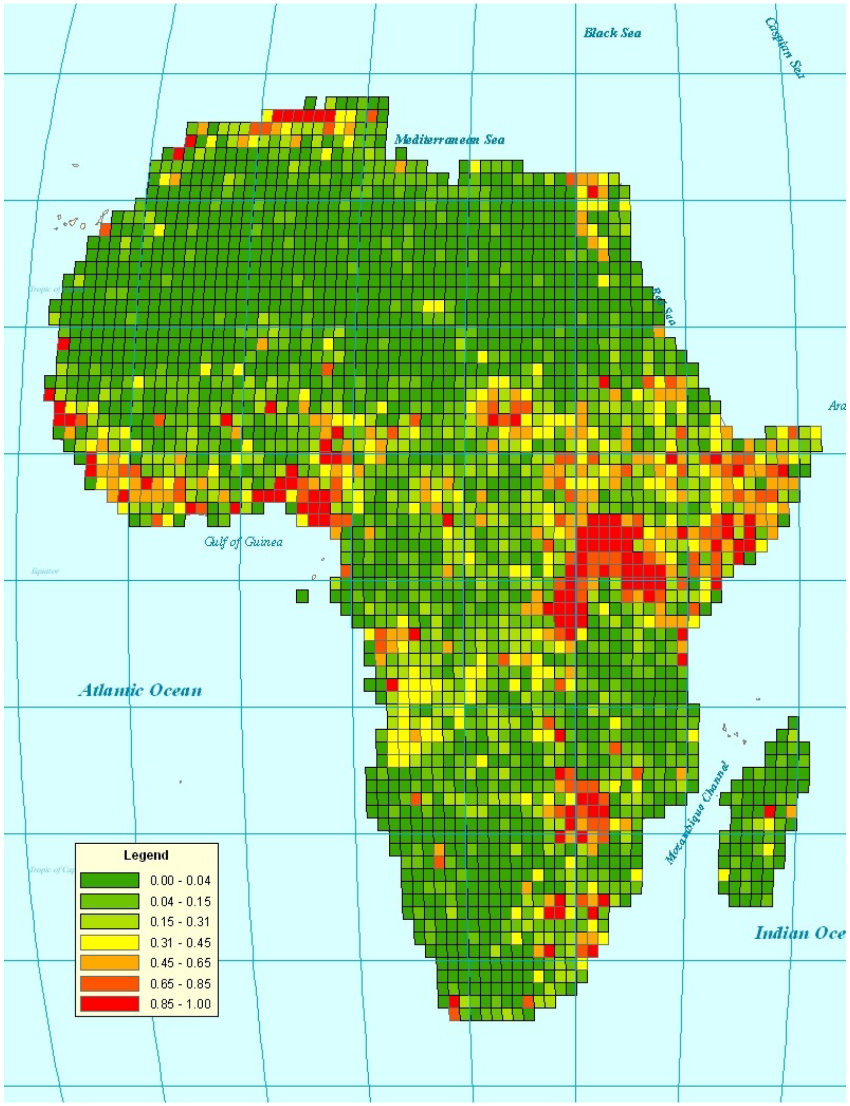

Figure 1A:

Fraction of years with at least one conflict event (1997-2011)

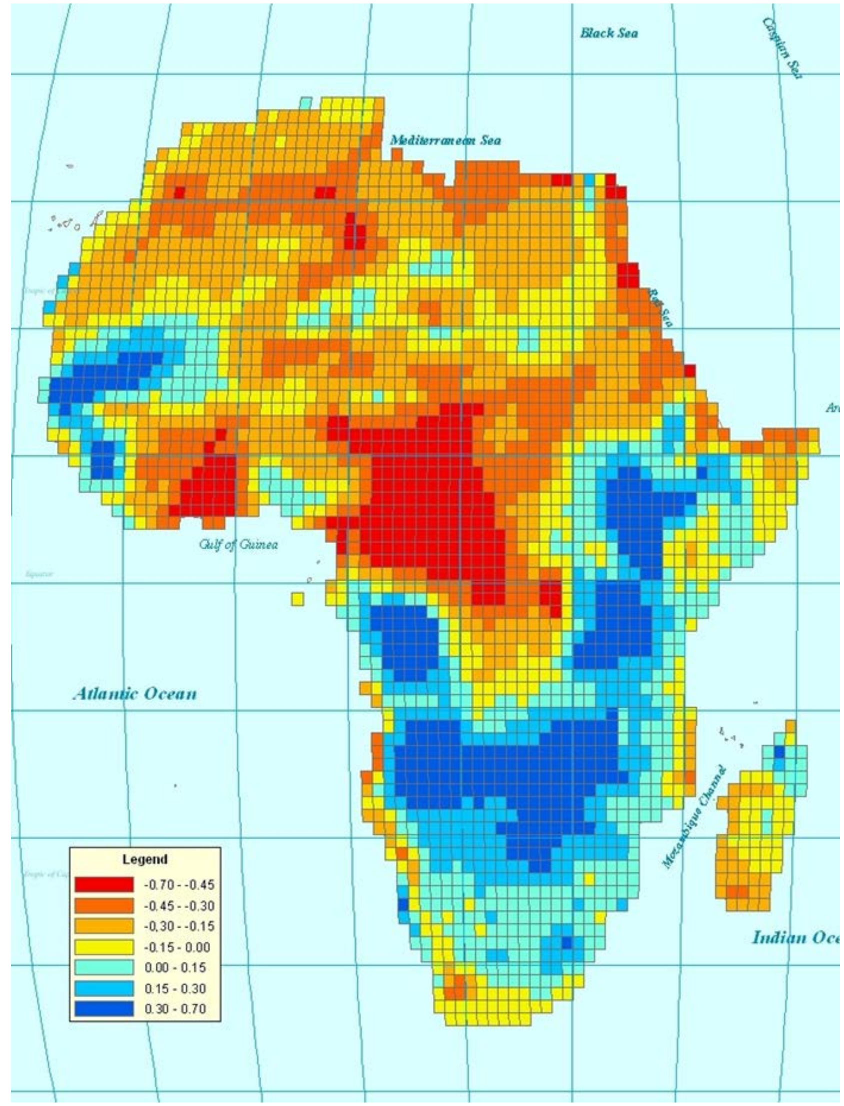

Figure 1B:

Average SPEI (1997-2011)

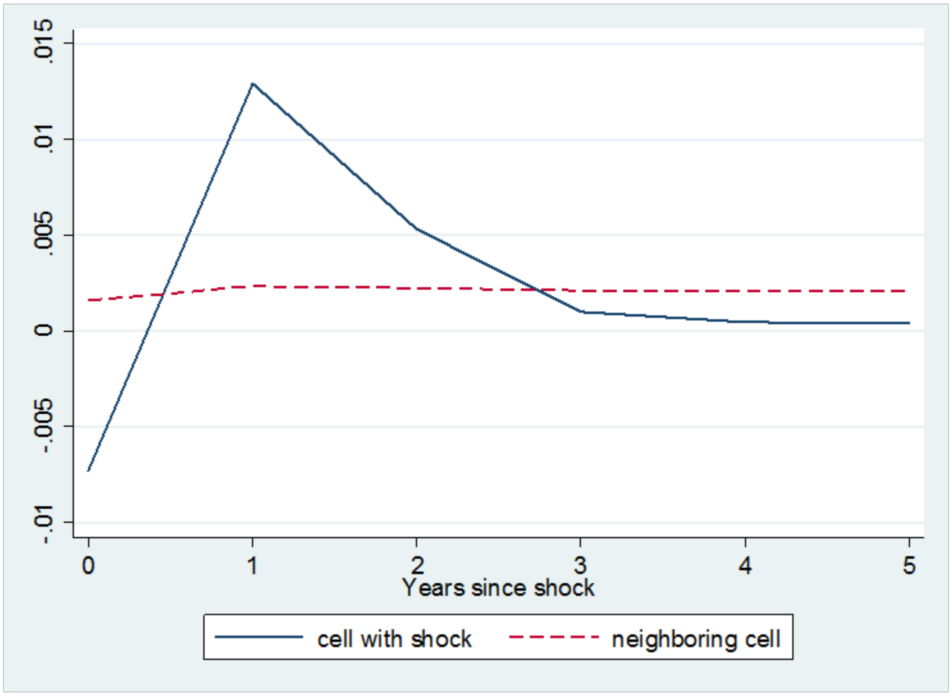

Figure 2a:

Dynamic impact of a one-time SPEI Growing Season shock on conflict incidence

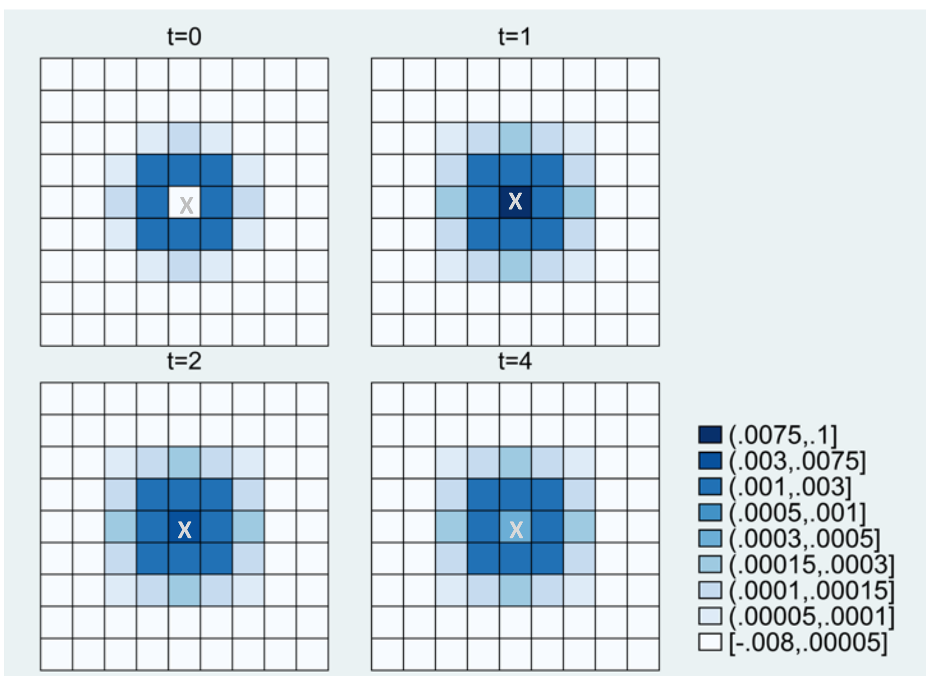

Figure 2b:

Spatial impact of a one-time SPEI Growing Season shock on conflict incidence

Appendix

A. Data sources

Our dataset covers 46 African countries over the period 1997 through 2011. The countries are Algeria, Angola, Benin, Botswana, Burkina Faso, Burundi, Central African Republic, Cameroon, Chad, Congo, Democratic Republic of the Congo, Cote d'Ivoire, Egypt, Equatorial Guinea, Eritrea, Ethiopia, Gabon, Ghana, Guinea, Guinea Bissau, Kenya, Lesotho, Liberia, Libya, Madagascar, Malawi, Mali, Mauritania, Morocco, Mozambique, Namibia, Niger, Nigeria, Rwanda, Senegal, Sierra Leone, Somalia, South Africa, Sudan, Swaziland, Tanzania, Togo, Tunisia, Uganda, Zambia, and Zimbabwe.

Conflict events

Data on civil conflict episodes are drawn from the PRIO/Uppsala Armed Conflict Location and Event (ACLED) dataset in its Fall 2012 version, covering the period 1997 through 2011. This is the most detailed conflict dataset developed by PRIO/Uppsala. It codes exact location in terms of latitude and longitude, date, and additional characteristics of a wide range of conflict-related events in all African states. Civil conflict episodes are defined broadly, to include not only battles with more than 25 casualties (the standard PRIO threshold) but all kinds of activity involving rebels, such as recruitment or the establishment of headquarters. Event data are derived from a variety of sources, mainly concentrating on reports from war zones, humanitarian agencies, and research publications. Information from local, regional, national, and continental media is reviewed daily; consistent NGO reports are used to supplement media reporting in hard-to-access cases; and Africa-focused news reports are integrated to supplement daily media reporting (Raleigh et al., 2012). The result is the most comprehensive and wide-reaching source material currently used in disaggregated conflict event coding.

For robustness, we also consider the alternative Uppsala Conflict Data Program Georeferenced Event Dataset version 2.0 (UCDP-GED). GED is comparable to ACLED in its spatial and temporal resolution, as it covers all of Africa for the period 1989-2014, and in its structure, in that the unit of observation is the conflict event, geocoded with latitude and longitude. It is, however, more restrictive than ACLED in the definition of events, designated in GED as incidents "where armed force was used by an organized actor against another organized actor, or against civilians, resulting in at least 1 direct death at a specific location and a specific date" (Sundberg & Melander, 2013). Moreover, such events are recorded only for conflicts that reach at least 25 battle-related deaths per year, according to the standard PRIO threshold. Another difference with ACLED lies in the underlying data collection process. GED events are coded following a two-step process, by which global newswire sources are consulted first, and then confirmed consulting local/specialized sources, such as translations of local news performed by the BBC, local media, NGO reports, and field reports.

Crop data

Data on the geographical distribution of agricultural crops is drawn from the M3-Crops Data by Monfreda, Ramankutty, and Foley (2008), a detailed raster dataset at the 5 arc minutes $\times$ 5 arc minutes resolution (about 9.2 km $\times$ 9.2 km at the equator) that includes 137 crops. For each 5'$\times$5' cell in the raster and each of the 137 crops included, Monfreda, Ramankutty, and Foley (2008) report harvested area in hectares. We aggregate the harvested area variable at the lower resolution of our dataset (i.e., 1 degree $\times$ 1 degree) and we employ it to rank the crops cultivated in each cell. We identify the main crop for each cell of our dataset as the crop with the largest harvested area in the cell; we thus obtain 30 different “main crops” in our full sample. While our main analysis relies on information on the growing season for the main crop, for robustness we also identify the second and third crops by harvested area, and we employ this information to construct a weighted growing season indicator based on the first three crops in a cell.

Natural resources

In an effort to collect georeferenced data on as many natural resources as possible, data on the location of mineral resources are drawn from a combination of the Mineral Resource Data System (MRDS) prepared by the United States Geological Survey (USGS) and the PRIO/Uppsala datasets Gemdata, Petrodata, and Diadata. We have identified 85 types of mineral commodities present in the countries of our dataset, including precious metals, industrial metals, oil, and gems.

PRIO natural resources datasets were compiled through an intensive literature search of academic databases and journals, national geological survey reports, and industry databases and reports, and as a result they tend to be more comprehensive and reliable than USGS. However, although likely to underreport mineral occurrences, USGS data are the only comprehensive, georeferenced data source for mineral commodities available to the general public.

Ethnic groups

Data on ethnic groups are drawn from the new University of Zurich “Geo-referencing of Ethnic Groups” (GREG) dataset (Weidmann, Rød, & Cederman, 2010). It relies on maps and data drawn from the classical Soviet Atlas Narodov Mira and employs geographic information systems to represent group territories as polygons.[1] We used the maps available in the GREG data and combined them with our raster grid to measure the extent of ethnic diversity in each cell. As a proxy for ethnic grievances, we compute a cell-level ethno-linguistic fractionalization (ELF) index, based on the shares of inhabited territory attributed to different ethnic groups in each cell.

In order to identify the presence in a cell of discriminated groups, we consult the Geo-referencing Ethnic Power Relations (GeoEPR-ETH) dataset (Wucherpfennig et al., 2010). The GeoEPR-ETH dataset provides georeferenced information on politically relevant ethnic groups, classified by their access to political power. We focus on ethnic groups classified as “discriminated”- that is, whose members are “subjected to active, intentional, and targeted discrimination, with the intent of excluding them from both regional and national power”(Wucherpfennig et al., 2010). In order to alleviate reverse causality concerns, we consider the power status of ethnic groups at the beginning of the sample period. We then compute the number of discriminated groups whose homelands overlap with a given cell.

Geography and infrastructure[2]

[1] Other definitions of ethnic groups (e.g. that used by James Fearon) cannot be used in our setting as, to the best of our knowledge, there is no georeferenced source that would allow us to map them at the high level of spatial disaggregation we are using.

[2] In a previous version of the paper, all variables related to geography and infrastructure were drawn from the Yale G-Econ Gridded Output dataset. In the current version, all of these variables have been recomputed using updated sources.

By overlaying our grid with country borders (as of 2012) we derive several control variables. The dummy *Shared* equals 1 if a cell contains a state border and 0 otherwise. The dummy *Border* equals 1 if a state border overlaps with one of a cell's sides (as would be the case for borders traced in correspondence to integer values of latitude or longitude) and 0 otherwise. Finally, we assign country fixed effects based on the country to which the majority of a cell belongs. We also compute the area, in squared kilometers, of each cell corresponding to land (i.e. excluding sea or lakes).

In order to investigate at the disaggregated scale the relationship between mountainous terrain and conflict, we include two different measures: one is the average elevation in a cell and one is a cell-level roughness indicator; both are measured in meters. The roughness indicator we employ is the topographic ruggedness index developed by Riley, DeGloria, and Elliot (1999) and used by, among others, Nunn and Puga (2012). It captures the average elevation change between adjacent points in a digital elevation grid within a cell; as such, it is able to capture topographic irregularities rather than elevation levels. The underlying elevation data is drawn from the Shuttle Radar Topography Mission (SRTM), which has an original grid resolution of 3 arc seconds.

Data on the location of roads are drawn from the Global GIS Atlas developed by the U.S. Geological Survey, a digital atlas of the world at a nominal scale of 1:1 million. These data have no time variation and report only the roads known in year 2000. To mitigate measurement error and selection concerns, we use as a proxy for road density a dummy for the presence in the cell of at least one road of primary use.

We also compute the distance from the closest major navigable river - measured in kilometers from the cell's midpoint - to capture the strategic importance of the location. A map of major rivers in Africa is drawn from the Environmental Systems Research Institute (ESRI).

Climate data

Our main climate indicator is the Standardized Precipitation-Evapotranspiration Index (SPEI), a recently developed multiscalar drought index (Vicente-Serrano et al., 2010). These authors use data on temperature and precipitation from CRU TS3.0 as inputs into SPEI. However, CRU TS3.0 relies on gauge data, and this has some shortcomings in the context of our analysis. The first is that given the limited number of stations in Africa, a significant amount of interpolation needs to be done in order to produce the data at the fine level of disaggregation we are using. This interpolation may artificially generate patterns of spatial correlation in weather shocks, thus hampering our ability to estimate the "true" extent of interdependency. The second potential problem is that the availability of gauge data may itself be endogenous to conflict. To deal with the above problems we chose to manually recalculate the SPEI index, feeding in the formula data on temperature, precipitation, and other atmospheric variables during 1979 through 2011 drawn from the ERA-Interim dataset (Dee et al., 2011) created by the European Centre for Medium-Range Weather Forecasts (ECMWF).[3] The ECMWF ERA-Interim archive provides reanalysis data available at a variety of grid resolutions, and with temporal resolution of up to 6 hours, for the period 1979 through 2011. Data are elaborated starting from high-frequency observations from a variety of sources, including weather stations, satellites, and sondes. ERA-Interim is considered a very high-quality dataset, and represents a significant improvement over gauge data in areas with sparse weather stations such as Africa. In fact, it is important

[3]A previous version of the paper featured the SPEI series as originally proposed by Vicente-Serrano et al. (2010). Results are available upon request.

for us not to rely exclusively on raw gauge data for two reasons. First, given the limited number of stations in Africa, a significant amount of interpolation would be needed, which may artificially generate patterns of spatial correlation in weather shocks. Second, the availability of gauge data may itself be endogenous to conflict.

The SPEI index is expressed in units of standard deviation from the average based on the available period (1979-2011). The data is fitted to a log-logistic distribution and normalized to a flexible multiple time scale such as 1, 4, 6, 12, 24, 48 months, etc. A short (say, 4 months) time scale reflects short- and medium-term moisture conditions and thus provides a seasonal estimation of precipitation as it is relevant for agriculture. For this reason, we use SPEI at a 4-month time scale. Details on the computation of SPEI are in section B.

In some of our specifications we also consider precipitation and temperature individually, both drawn from ECMWF ERA-Interim.

For our forecast exercise, we compute projected SPEI using monthly projected values of total precipitation, maximum temperature, and minimum temperature during 2016 through 2050. Climate projections are generally derived through general circulation models (GCMs), which simulate future climate outcomes under a set of standardized assumptions on future human activity or "emissions scenarios." Following the recommendations of Auffhammer et al. (2013) and Burke et al. (2015), we perform our forecast exercise using projections obtained with several climate models and under different emissions scenarios (all of which meet Intergovernmental Panel on Climate Change standards).

All of the projection data we employ are drawn from the World Climate Research Programme's (WCRP's) Coupled Model Intercomparison Project phase 5 (CMIP5) multi-model dataset (Meehl, Stouffer, & Taylor, 2012), a set of coordinated climate model experiments. In particular, we employ downscaled gridded data at a resolution of 0.5 degree from the Downscaled CMIP3 and CMIP5 Climate and Hydrology Projections. These projections are provided for four possible scenarios about future anthropogenic greenhouse gas (GHG) emissions, measured by representative concentration pathways (RCPs). In particular, RCP 2.6 assumes that global annual GHG emissions peak between 2010 and 2020, and decline substantially thereafter; RCP 4.5 assumes that the peak is around 2040, while RCP 6 assumes that they peak around 2080; finally, RCP 8.5 assumes that emissions continue to rise throughout the 21st century (Meinshausen et al., 2011).

We present results obtained using projections from three of the models in the CMIP5: FGOALS-G2 (Flexible Global Ocean-Atmosphere-Land System Model, grid-point version 2), developed by the Chinese Academy of Sciences and Tsinghua University (Li et al., 2013); EC-EARTH, developed by a consortium of 29 European research institutions working in partnership with ECMWF; and FIO-ESM (First Institute of Oceanography-Earth System Model; Quiao et al., 2013). For each model, we report all the emission scenarios considered. Details on how projected SPEI is computed using these input data are provided in Section B.

Crop calendars and crop-specific climate shocks

We construct specific indicators for climatic conditions during the growing season, which is when crops are most sensitive to unfavorable conditions. To retrieve the growing season of the main crop (ranked by harvested area) cultivated in each cell we rely on crop calendars drawn from a variety of sources.

As a primary source, we use the Global Monthly Irrigated and Rainfed Crop Areas around the year 2000 (MIRCA 2000), prepared by the Physical Geography Department of the Goethe Universität Frankfurt am Main (Portmann, Siebert, & Döll, 2010). This is a dataset of monthly growing seasons of 26 irrigated and rain-fed crops at different latitudes and longitudes, with a spatial resolution of 5 arc-minutes $\times$ 5 arc-minutes. It is our preferred source given that it disaggregates by irrigated and rain-fed crops - which we focus on - and given its high spatial resolution.

For the crops and cells not covered by MIRCA, we turn to two complementary sources, which both report crop calendars at the country level. The first are those generated with the Food and Agricultural Organization (FAO) Food security and Early warning Network for Information eXchange Workstation (FENIX) Crop Calendar tool. The FENIX tool indicates for various crops and countries the planting and harvesting season. We define the growing season as the months between planting and harvesting. Our second source is the FAO Seeds and Plant Genetic Resources Crop Calendars.

Our key climate variable, denoted as *SPEI Growing Season*, is computed by averaging monthly SPEI over the growing season months of a cell's main crop in a given year. As a reference, the correlation between SPEI in the growing season and outside the growing season is 0.64. For rainfall, this figure is 0.32. The correlation between the growing season dummy for main and second crop is 0.64.

Country-level variables

The tax to GDP ratio, measured at the country-year level, is drawn from Cagé and Gadenne (2014), who combine Mitchell (2007)'s International Historical Statistics, the Baunsgaard and Keen (2010) dataset, and the International Monetary Fund's Government Finance Statistics.

The Polity IV combined polity score is drawn from the Polity IV Project dataset (Marshall, Jaggers, & Gurr, 2014), a widely used source of cross-national, longitudinal data on the authority characteristics of polities 1800 through 2010. This dataset provides a number of ordinal-scale indicators derived from expert codings of factors such as the competitiveness of political participation and the openness and competitiveness of executive recruitment. The combined polity score is computed by subtracting the Autocracy score from the Democracy score. It ranges from $+10$ (strongly democratic) to -10 (strongly autocratic). The Democracy score is an additive eleven-point scale derived from codings of the competitiveness of political participation, the openness and competitiveness of executive recruitment, and constraints on the chief executive. The Autocracy score is constructed similarly, based on codings of the competitiveness of political participation, the regulation of participation, the openness and competitiveness of executive recruitment, and constraints on the chief executive.

B. The Standardized Precipitation-Evapotranspiration Index (SPEI)

Most studies related to drought analysis and monitoring systems have resorted to the Palmer Drought Severity Index (PDSI), based on a soil-water balance equation, or the Standardized Precipitation Index (SPI), based on precipitation. One of the limitations of the PDSI index is its fixed temporal scale (between 9 and 12 months) and an autoregressive property by which PDSI values are affected by the conditions up to four years in the past (Vicente-Serrano et al., 2010). Precipitation-based drought indices like SPI, on the other hand, assume that temperature and potential evapotranspiration have negligible variability compared to precipitation. This makes such indexes unsuitable to identify the role of global warming in future drought conditions.

Our manual recalculation of SPEI uses the R routines developed by Vicente-Serrano et al. (2010). Due to the probabilistic nature of the SPEI index, it is recommended to use the longest sample possible in its computation. We thus consider the entire ERA-Interim available sample (1979-2011). The computation involves the following steps:

1) Compute climatic water balance, defined at the monthly level as the difference D between precipitation and potential evapotranspiration (PET).

Since no direct data on PET is usually available, SPEI is based on an approximation. A number of equations exist to model PET based on available data. In our 1979-2011 sample we make use of the FAO-56 Penman-Monteith equation described in Allen et al. (1998), which is recommended by FAO as the best method for determining reference evapotranspiration. The original parameterization is used, corresponding to a short reference crop of 0.12 m height:

$$PET = \frac{0.408(R_n - G) + \gamma \frac{900}{T+273} u_2 (e_s - e_a)}{\Delta + \gamma(1 + 0.34 u_2)}$$

where R_n is the net radiation at crop surface, G is the soil heat flux density, T is the mean daily air temperature at 2m height, e_S is saturation water pressure, e_a is actual vapor pressure, Δ is the slope of the vapor pressure curve, and γ is the psychometric constant. Given that many of these inputs are seldom available, chapter 3 of Allen et al. (1998) provides methods to compute the missing variables based on available data. For instance, incoming solar radiation can be estimated based on sunshine duration or percent cloud cover. Similarly, saturation water pressure can be estimated from the dew-point temperature. If unavailable, the atmospheric surface pressure required for computing the psychrometric constant can be assumed to be constant. The inputs we use to approximate the Penman equation in our 1979-2011 sample are average temperature, average maximum and minimum daily temperatures, dewpoint temperature, cloud cover, sunshine duration, and wind speed.

2) The calculated difference D between precipitation and PET is aggregated at different time scales, as for the SPI. This is achieved by applying a kernel function to the data, which allows the incorporation of information from previous time steps into the calculation of the current step. We use a Gaussian kernel, allowing data from the past to have a decreasing influence in the current step as the temporal lag between current and past steps increases.

3) Finally, the time series is standardized according to a log-logistic distribution, whose parameters are estimated by the L-moment procedure. The probability distribution function of D according to the log-logistic is

$$F(x) = \left[1 + \left(\frac{\alpha}{x - \gamma}\right)^{\beta}\right]^{-1}$$

SPEI is calculated as the standardized values of $F(x)$. By construction, it has mean 0 and standard deviation 1 in a given location over the historic sample - in our case 1979 through 2011. As shown in the summary statistics table, the average of SPEI within our estimation sample 1997 through 2011 is actually below 0 because of a trend toward drier climate.

SPEI projections

For our forecast exercise, we use cell-level projections of total precipitation, maximum temperature, and minimum temperature for years 2016 through 2050 to construct a projected version of our SPEI-based indicator. Our data sources are documented in Section A of this Appendix.

The first step in our calculation involves using projections of future precipitation and temperature to compute future projected water balance. Due to more limited data availability, in this exercise PET is approximated with the less demanding Hargreaves equation (Hargreaves, 1994) instead of the Penman equation:

$$PET = 0.00203 \cdot R_a \cdot (\frac{(T_{\max} + T_{\min})}{2} + 17.8) \cdot (T_{\max} - T_{\min})^{0.5}$$

where R_a is mean external radiation and $T_{\max}$ and $T_{\min}$ are the mean daily maximum and minimum temperatures at 2m height. Mean external radiation is estimated from the latitude and the month of the year.

The rest of the calculation follows the steps detailed above.

Note that SPEI is by construction a standardized measure, with mean 0 and standard deviation 1 in the reference sample, which in our main analysis is 1979 through 2011. When we forecast future SPEI we standardize it over the full range of available actual and projected rainfall and temperature data (i.e., 1979 through 2100). By standardizing over the period 1979 through 2100 (in which temperatures are rising) rather than over 1979 through 2011, in the projected version of SPEI a negative SPEI value corresponds to a more severe drought in absolute terms than a comparable value in the historical sample we use for the main analysis. Therefore, we are being relatively conservative in our strategy, implying that our estimated impacts may be smaller than if we standardized over a shorter horizon.

C. Derivation of the likelihood for dynamic spatial panels[4]

Our preferred specification is a dynamic, spatially autoregressive Durbin model (Elhorst, 2009) in which we let conflict in one cell depend on lagged conflict in the cell itself, on contemporaneous conflict in the neighboring cells, and on a set of covariates measured in the cell itself and in the neighboring cells. An obvious identification challenge is posed by the endogeneity of the first two regressors, which requires these models to be estimated either by GMM or maximum likelihood. We use the routines developed by Hughes (2012) and Belotti, Hughes, and Mortari (2016), which are based on quasi-maximum likelihood techniques described in Elhorst (2009), Parent and LeSage (2012), and Yu, de Jong, and Lee (2008). In this section we derive the likelihood function for a benchmark dynamic spatial model, illustrating how this can address the simultaneity deriving from the autoregressive terms, following the exposition of Parent and LeSage (2009).

Consider the following dynamic, spatial, random effects model with N cross-sectional units and T time periods:

$$y_t = \phi y_{t-1} + \rho W y_t + i_N \alpha + x_t \beta + \eta_t \tag{1}$$

with $\eta_t = \mu_t + \varepsilon_t$, where $y_t = (y_{1t}, \ldots, y_{Nt})'$ is the $N \times 1$ vector of observations for the t-th time period, α is the intercept, i_N is an $N \times 1$ column vector of ones, x_t is the $N \times k$ matrix of non-stochastic regressors and μ is an $N \times 1$ vector of random effects, with $\mu_i \sim N(0, \sigma_\mu^2)$. The random terms ε_t are i.i.d. with zero mean and a variance $\sigma_\varepsilon^2 I_N$, and μ is assumed to be uncorrelated with ε_t. W is a row-normalized, symmetric $N \times N$ spatial weighting matrix with zeros on the diagonal, whose eigenvalues are denoted as $\varpi_i, i = 1, \ldots, N$. For simplicity spatial lags of the covariates are not explicitly included in (1), but they could be part of matrix x_t.

[4]This section draws on Parent and Le Sage (2012).

The basic idea is to remove the two sources of autocorrelation by combining two transformations: a space filter to remove the spatially autoregressive term and a time filter á la Prais-Winsten to remove the temporal autoregressive one.

Define first the space filter as the $N \times N$ matrix:

$$B = I_N - \rho W \tag{2}$$

To see how this transformation removes the spatial autoregressive term, suppose that $\phi = 0$ and apply this filter to equation (1):

$$By_t = i_N \alpha + x_t \beta + \eta_t \tag{3}$$

Now define the time filter as the $T \times (T+1)$ matrix

$$C = \begin{bmatrix} -\phi & 1 & 0 & ... & 0 \\ \vdots & \ddots & \ddots & \ddots & \vdots \\ 0 & ... & ... & -\phi & 1 \end{bmatrix} \tag{4}$$

To see how this transformation removes the temporal autoregressive term, consider the $(T+1) \times 1$ vector of observations for the i-th cross-sectional unit $y_i = (y_{i0,}\ ...,\ y_{iT})'$. Similarly, let $x_i = (x_{i1,}\ ...,\ x_{iT})'$ be the $T \times k$ vector of covariates observed in the i-th cross-sectional unit and $\eta_i = (\eta_{i0,}\ ...,\ \eta_{iT})'$ a vector of errors. Further assume that $\rho = 0$. Applying the filter to y_i one obtains:

$$Cy_i = i_T \alpha + x_i \beta + \eta_i \tag{5}$$

Note that we are assuming that y_0 is given. This considerably simplifies the computational complexity of the estimation and has been shown to have little effect on the estimates when T is not too small.

The space-time filter proposed by Parent and LeSage is given by the Kronecker product of matrices C and B. Set $Y = (y_0', ..., y_T')'$ and $X = (x_1', ..., x_T')'$ and apply the filter to the entire vector of observations. One obtains:

$$(C \otimes B)Y = X\beta + i_{NT}\alpha + \eta \tag{6}$$

with $\eta \sim N(0, \Omega)$.

Since the random effects are integrated out, the $NT \times NT$ variance-covariance matrix can be shown to be equivalent to

$$\Omega = \sigma_\mu^2 (J_T \otimes I_N) + \sigma_\varepsilon^2 [I_T \otimes I_N] \tag{7}$$

with $J_{T+1} = i_{T+1} i_{T+1}'$.

This allows the log-likelihood for the complete sample size of T for the model defined in (1) to be written as

$$\ln L_T(\xi) = -\frac{NT}{2} \ln(2\pi) - \frac{1}{2} \ln |\Omega| + T_{i=1}^N \ln[(1 - \rho\varpi_i)] - \frac{1}{2} \eta' \Omega^{-1} \eta \tag{8}$$

where $\xi = (\beta', \alpha, \sigma_\varepsilon^2, \sigma_\mu^2, \phi, \rho)$.

The Stata *xsmle* command we use extends this technique to fixed effects models, implementing the procedure described by Yu, de Jong, and Lee (2008).

D. Cross-sectional estimates

In this section we explore the empirical determinants of civil conflict, focusing on time-invariant characteristics such as geography and location of mineral deposits. Our interest in conducting this type of analysis hinges on two factors. First, despite the limitations of cross-sectional inference, the high level of spatial resolution of our data limits the concerns related to state-wide unobservable determinants of conflict. Second, the data exhibits spatial dependence, in the sense that geographic features in a given cell may affect neighboring cells: this potentially yields interesting insights on the interdependence among neighboring locations in the diffusion of conflict.

Econometric models

We collapse our cell/year observations to create a time-invariant measure of conflict prevalence in a given cell. Our dependent variable is the fraction of years in the sample in which the cell has experienced at least one conflict event, denoted as $\overline{ANY\ EVENT}$. Consider a cross-section of N cells, each denoted by c and located in country i. Let X be a vector of time-invariant controls (e.g., terrain characteristics) and μ a vector of country fixed effects. We estimate three models:

$$\overline{ANY\ EVENT}_{c,i} = \alpha + \delta X_c + \mu_i + \varepsilon_{c,i} \tag{9}$$

$$\overline{ANY\ EVENT}_{c,i} = \alpha + \delta X_c + \lambda W \cdot X + W \cdot \mu + \varepsilon_{c,i} \tag{10}$$

which are estimated by OLS with Conley (1999) errors, and

$$\overline{ANY\ EVENT}_{c,i} = \alpha + \varphi W \cdot \overline{ANY\ EVENT} + \delta X_c + \lambda W \cdot X + W \cdot \mu + \varepsilon_{c,i} \tag{11}$$

estimated by maximum likelihood with errors clustered by cell.

Results

Summary statistics for the cell-level characteristics included in vector X are reported in Table A1. The territory in our sample appears to be mineral rich, as 21 percent of the cells have at least one mineral deposit, and on average moderately elevated, with an average elevation of 594 meters. Local ethnic fractionalization appears to be moderate, with an average cell-level ELF index of 0.2. We include among our cross-sectional controls a *Shared* dummy for cells that do not belong entirely to one country but contain a country border; these cells are about 38 percent of our sample. The dummy *Border*, on the other hand, identifies cells whose edge coincides with a state border (about 4 percent of our sample).

Our cross-sectional evidence is presented in Table A2. The table reports OLS coefficients and standard errors in parentheses corrected for spatial dependence following Conley (1999). The dependent variable captures average conflict incidence with a mean and standard deviation of, respectively, .17 and .25.

In columns 1 and 2 we consider "own" characteristics of the cell (Model I), in columns 3 and 4 we also include characteristics of the neighboring cells (Model II), and in columns 5 and 6 (Model III) we estimate a spatial lag model in which we further include a spatially autoregressive component to capture direct conflict spillovers across neighbors. Neighbors are defined according to our benchmark weight matrix as cells whose midpoints lie within 180 km of the midpoint of the own cell. Columns 1, 3, and 5 report the coefficients of a purely cross-sectional regression without area fixed effects. In columns 2, 4, and 6 we instead report our preferred specification that includes country fixed effects (and their spatial lags, for columns 4 and 6).

The first set of controls we include measure geo-administrative characteristics: *Shared* is a dummy for whether a cell belongs to more than one country, and *Border* is a dummy for whether a cell's side is tangent to a country border (the two are not mutually exclusive). The coefficient for *Shared* is positive and significant in all specifications; that for *Border* is negative and significant. One potential explanation is the spurious correlation between *Border* and the presence of deserts (arbitrary borders placed in correspondence to integer latitude and longitude are mostly found in desertic areas). The third (insignificant) control listed in the table, *Area*, measures the area of the cell corresponding to land, to account for coastal cells that correspond mostly to sea.

We next move to geographic characteristics of the terrain. *Elevation* measures the average altitude of the cell (in meters), whereas *Rough* captures terrain ruggedness. Both coefficients are positive in all specifications, consistent with previous literature finding that impervious areas provide safe havens for rebels (e.g., Fearon and Laitin, 2003). *Distance to river* is the minimum distance (in km) of the centroid of the cell from a navigable river and does not appear to be systematically associated with conflict.

Transport infrastructure plays a significant role, as confirmed by the coefficient of the variable *Road*, which is a dummy equal to 1 if the cell contains at least one road of "primary use" (as defined by the Global GIS Atlas). The positive relationship with conflict is consistent with two interpretations: areas served by main roads are easier to reach for the purpose of attacks, and the benefits of capturing those areas are higher.

We next turn to some of the channels more widely explored in the cross-country literature. The first is ethno-linguistic fractionalization (ELF), which is computed using the relative territory shares occupied by each group as per GREG, after having normalized these shares by the total inhabited land in each cell. The average cell in our sample has about two ethnic groups, with an ELF index of 0.2. The coefficient of this variable is positive in all specifications, although significance varies. This is consistent with ethnic diversity being associated with "grievance" motives for conflict.

The second channel is linked to the natural resource curse. The variable *Minerals* is a dummy equal to 1 if the cell contains at least one mineral deposit (21 percent of the cells in our sample have at least one such deposit). All else being equal, the presence of minerals in the cell is associated with a significantly higher incidence of conflict, in the order of about one-fourth of a standard deviation of the dependent variable. The effect could be due to "greed" as well as to a revenue effect from mineral resources that rebels and government can use to finance military activities.

Neighbors' characteristics are represented by the spatial lags of the covariates considered above. Most neighbors' characteristics are statistically insignificant or very close to 0, suggesting that, in general, the impact of the geographic characteristics discussed above is a strictly local one.

Finally, when we consider conflict spillovers the coefficient of the autoregressive term $W \cdot Y$ in columns 5 and 6 is positive and highly significant. Based on the estimate in column 6, a cell that had one of its neighbors experiencing conflict for the entire sample period is in conflict for 0.066 more years, which is one-fourth of a standard deviation. Considering that the average number of neighboring cells in our sample is 7.4, a cell surrounded by neighbors that *all* had conflict throughout the period would be in conflict for 0.48 more years; that is two standard deviations. Note that, however, this analysis employs a definition of conflict prevalence with no time variation: this should be taken only as suggestive evidence that conflict spillovers in space are relevant, as only the panel analysis can provide adequate estimates of both temporal and spatial spillovers.

In Table A3 we repeat the analysis disaggregating the dependent variable by type of conflict event.

E. Additional results

Instrumental variable estimates

Table A4 reports two instrumental variables versions of Model III. In column 4 we instrument for conflict in the immediate neighbors using conflict in the second-order neighbors - an approach similar to those used in time series to address autocorrelation in the dependent variable. In column 7 our instrument for conflict in the immediate neighbors is the growing season SPEI of second-order neighbors - an approach similar to that employed by Bramoullé, Djebbari, and Fortin (2009) to address peer effects. In both cases we instrument lagged conflict in the own cell using the second lag of conflict, again following the time series literature. First-stage estimates for the two endogenous variables are reported in columns 2 and 3 for the first IV specification and 5 and 6 for the second. Column 1 reports plain OLS estimates. Both instrumental variable approaches yield estimates that are comparable, in sign and significance, to those found in Table 2 of the main text. In terms of magnitudes, IV estimates for spatial and temporal spillovers appear larger, whereas the coefficient on or our main explanatory variable (*SPEI Growing Season*$_{t-1}$), appears to be very stable around 0.04.

Sensitivity of climate and conflict projections

In Table A5 we perform a sensitivity analysis of the results presented in section 4.2 of the paper. We explore sensitivity of our forecast results to different climate models and emissions scenarios, as recommended by Burke et al. (2015). We report averages of projected SPEI shocks (panel A) as well as averages of the marginal conflict increase predicted by such shocks (panel B) for a range of models and scenarios. We also report predictions obtained using estimates from the simpler non-spatial and non-dynamic model I (panel C). Our estimates are remarkably stable across climate models and scenarios.

Heterogeneous spatial spillovers of shocks

In Table A6 we explore the extent to which weather shocks in different types of neighbors differentially affect conflict likelihood in the own cell. These specifications differ from our benchmark in that we consider different sets of neighbors within the same regression for the purposes of defining the spatial lags of *SPEI Growing Season.* In each column, the weighting matrices W_1 and W_2 correspond to two mutually exclusive sets of neighbors, defined in the header (for example, same main ethnic group vs. different main ethnic group; same main crop vs. different main crop; etc.). The exclusion restriction is, as in our benchmark estimates, that weather shocks occurring among the second-order neighbors are not directly affecting conflict other than through spillovers.

Motivated by the importance of ethnic ties in providing insurance against economic shocks, we focus on two potential sources of heterogeneity: ethnicity and crop diversification (proxied by whether a neighboring cell shares the same main crop). If there is coinsurance within ethnic boundaries, a shock occurring within the homeland is less likely to translate into conflict, as the insurance network will neutralize its effect on income. However, if there is crop specialization (as opposed to diversification), the ability to coinsure may be limited and a shock to neighbors, coethnics or otherwise, may increase conflict likelihood in the own cell too. Results in Table A6 suggest that only shocks occurring among coethnic neighbors and among neighbors cultivating the same main crop increase conflict in the own cell. This provides suggestive evidence that coinsurance within the ethnic group may not be effective, possibly due to specialization, and that uniformity in crop patterns across space may prevent insurance across neighbors.

Conflict onset and termination

In Table A7 we consider conflict onset and termination as dependent variables. The results of this exercise are discussed in section 5.5 of the paper and offer suggestive evidence that SPEI shocks may be local triggers of new conflicts.

Sensitivity to spatial scale and spatial weighting matrixes

In Tables A8 and A9 we explore the sensitivity of our benchmark estimates to, respectively, different grid resolutions and different spatial weighting matrixes. Results are discussed in section 6.1 of the paper and validate our choice of benchmark grid resolution and weighting matrix.

Other climate indicators

In Table A10 we turn to other potential climate indicators. The heading of each column specifies which climate indicator is used in that specification. All estimates refer to Model III with cell fixed effects.

Column 1 considers a stand-alone SPEI indicator, averaged over the entire year. This does not appear to be a significant conflict predictor, suggesting that indeed what matters are climatic conditions during the growing season.

In column 2 we focus on drought spells. Our climate indicator, denoted as *SPEI Shock Growing Season*, is defined as follows: in a given year, consider the growing season of the main crop; take the number of consecutive growing season months in which SPEI was below its mean by more than one standard deviation; express this measure as a fraction of the number of growing season months. The resulting variable will range between 0 and 1, with 0 denoting a "good" year and 1 denoting a "bad" year in which the entire growing season witnessed abnormally low SPEI. Although not significant at conventional levels, the results indicate that abnormal shocks during the growing season are associated with greater conflict incidence the subsequent year.

In column 3 we investigate nonlinear effects of SPEI and augment our benchmark specification (from Table 2, column 5) with a quadratic term in *SPEI Growing Season*. The coefficients on the quadratic terms are small and insignificant.

In column 4 we consider an extended version of our benchmark *SPEI Growing Season* that includes the first three crops cultivated in each cell (instead of just the main one).[5] Results are qualitatively consistent with our benchmark, although not significant.

In columns 5 and 6 we turn to the two climate indicators that have been more widely employed in the cross-country literature: rainfall (measured in logs of yearly values, in millimeters) and temperature (in degrees centigrade). For each of these variables, we compute a "growing season indicator" obtained by averaging the monthly values over the growing season of the main crop. The coefficients on rainfall (column 5) have the expected negative sign, but they are typically insignificant. Those on temperature (column 6)

[5] More precisely, we consider a weighted average of *SPEI Growing Season*, where each of the three crops is weighted by its harvested area in the cell.

are also insignificant. The contrast with the existing literature, which finds significant effects of rainfall and temperature, may be rationalized by observing that our specification with both spatial and temporal lags of the dependent variable absorbs a lot of the variation in conflict, which is already reduced by the inclusion of cell fixed effects. The richness of SPEI - which embeds information on precipitation and temperature but also on latitude, month of the year, number of sunlight hours, etc. - allows us to get more precise estimates when we use our benchmark indicator.

Sensitivity to alternative conflict data

In Table A11 we consider an alternative conflict dataset, the UPCDP-GED dataset described in section A of this Appendix. Results of this sensitivity exercise are discussed in section 6.3 of the paper.

Alternative leads and lag structures

In Table A12 we consider specifications with different temporal lag structures, including leads of our main explanatory variable as a placebo test. Results of this exercise are discussed in section 6.3 of the paper.

References

[1] Anselin, Luc, *Spatial Econometrics: Methods and Models*, (Boston: Kluwer Academic, 1988).

[2] Auffhammer, Maximilian, Solomon M. Hsiang, Wolfram Schlenker, and Adam Sobel, "Using Weather Data and Climate Model Output in Economic Analyses of Climate Change," *Review of Environmental Economics and Policy* 7:2 (2013), 181-198.

[3] Baunsgaard, Thomas, and Michael Keen, "Tax Revenue and (or?) Trade Liberalization," *Journal of Public Economics* 94:9-10 (2010), 563-577.

[4] Belotti, Federico, Gordon Hughes, and Andrea Piano Mortari, "Spatial Panel Data Models using Stata," CEIS Tor Vergata Research Paper Series 14:5 (2016).

[5] Bramoullé, Yann, Habiba Djebbari, and Bernard Fortin, "Identification of Peer Effects Through Social Networks," *Journal of Econometrics* 150 (2009), 41-55.

[6] Burke, Marshall, John Dykema, David B. Lobell, Edward Miguel, and Shanker Satyanath, "Incorporating Climate Uncertainty into Estimates of Climate Change Impacts, with Applications to U.S and African Agriculture," *Review of Economics and Statistics* 97:2 (2015), 461-471.

[7] Cagé, Julia, and Lucie Gadenne, "Tax Revenues, Development, and the Fiscal Cost of Trade Liberalization, 1792-2006," working paper, Sciences Po and UCL (2014).

[8] Dee, Dick P., Sakari M. Uppala, Adrian J. Simmons, Paul Berrisford, Paul Poli, Shinya Kobayashi, Ulf Andrae, Magdalena Alonso Balmaseda, Gianpaolo Balsamo, Peter Bauer, Peter Bechtold, Anton Beljaars, Leo van de Berg, Jean Bidlot, Niels Bormann, C. Delsol, Rossana Dragani, Manuel Fuentes, Alan J. Geer, Leopold Haimberger, Sean B. Healy, Hans Hersbach, Elías Valur Hólm, Lars Isaksen, Per Kållberg, Martin Köhler, Marco Matricardi, A. P. McNally, Beatriz M. Monge-Sanz, Jean-Jacques Morcrette, B.-K. Park, Carole Peubey, Patricia de Rosnay, Christina Tavolato, Jean-Noël Thépaut, and Frederic Vitart, "The ERA-Interim Reanalysis: Configuration and Performance of the Data Assimilation System," *Quarterly Journal of the Royal Meteorological Society* 137:656 (2011), 553-597.

[9] Elhorst, J. Paul, "Spatial Panel Data Models" (pp. 377-407), in Manfred M. Fischer and Arthur Getis, eds., *Handbook of Applied Spatial Analysis* (Berlin: Springer-Verlag, 2009).

[10] FAO, FAOSTAT database, (faostat.fao.org/site/339/default.aspx), consulted 2014.

[11] Hughes, Gordon, "Implementing procedures for spatial panel econometrics in Stata," mimeo (2012).

[12] LeSage, James P., and Robert Kelley Pace, *Introduction to Spatial Econometrics* (Boca Raton, FL: CRC Press Taylor & Francis Group, 2009).

[13] Li, Lijuan, Pengfei Lin, Yongqiang Yu, Bin Wang, Tianjun Zhou, Li Liu, Jiping Liu, Qing Bao, Shiming Xu, Wenyu Huang, Kun Xia, Ye Pu, Li Dong, Si Shen, Yimin Liu, Ning Hu, Mimi Liu, Wenqi Sun, Xiangjun Shi, Weipeng Zheng, Bo Wu, Mirong Song, Hailong Liu, Xuehong Zhang, Guoxiong Wu, Wei Xue, Xiaomeng Huang, Guangwen Yang, Zhenya Song, and Fangli Qiao, "The Flexible Global Ocean-atmosphere-land System Model, Grid-point Version 2: FGOALS-g2," *Advances in Atmospheric Sciences* 30:3 (2013), 543-560.

[14] Marshall, Monty G., Keith Jaggers, and Ted Robert Gurr, "Polity IV Project, Political Regime Characteristics and Transitions, 1800-2010," www.systemicpeace.org/polity/polity4.htm, accessed 2014.

[15] Meehl, Gerald A., Ronald J. Stouffer, and Karl E. Taylor, "An Overview of CMIP5 and the experiment design," *Bulletin of the American Meteorological Society* 93 (2012), 485-498.

[16] Meinshausen, Malte, Steven J. Smith, Katherine Calvin, J. S. Daniel, Mikiko Kainuma, Jean-François Lamarque, Kenichi Matsumoto, Stephen A. Montzka, S. C. B. Raper, Keywan Riahi, Allison Thomson, Guus J. M. Velders, and Detlef van Vuuren, "The RCP Greenhouse Gas Concentrations and Their Extensions from 1765 to 2300," *Climatic Change* 109:1-2 (2011), 213-241.

[17] Mitchell, Brian R., *International Historical Statistics (Europe, the Americas, Africa, Asia, and Oceania)* (New York: Palgrave Macmillanl, 2007).

[18] Monfreda, Chad, Navin Ramankutty, and Jonathan A. Foley (2008), "Farming the Planet: Geographic Distribution of Crop Areas, Yields, Physiological Types, and Net Primary Production in the Year 2000," *Global Biogeochemical Cycles* 22 (2008), 1-19.

[19] Nunn, Nathan, and Diego Puga, "Ruggedness: The Blessing of Bad Geography in Africa", *Review of Economics and Statistics* 94:1 (2012), 20-36.

[20] Parent, Olivier, and James P. LeSage, "Spatial Dynamic Panel Data Models with Random Effects," *Regional Science and Urban Economics* 42:4 (2012), 727-738.

[21] Portmann, Felix T., Stefan Siebert, and Petra Döll, "MIRCA2000 - Global Monthly Irrigated and Rainfed Crop Areas around the Year 2000: A New High-resolution Data Set for Agricultural and Hydrological Modeling," *Global Biogeochemical Cycles* 24:1 (2010), doi:10.1029/2008GB003435.

[22] Qiao, Fangli, Zhenya Song, Ying Bao, Yajuan Song, Qi Shu, Chuanjiang Huang, and Wei Zhao, "Development and Evaluation of an Earth System Model with Surface Gravity waves," *Journal of Geophysical Research* 118:9 (2013), 4514-4524.

[23] Raleigh, Clionadh, Andrew Linke, Håvard Hegre, and Joakim Karlsen, "Introducing ACLED: Armed Conflict Location and Event Dataset," *Journal of Peace Research* 47:5 (2010), 1-10.

[24] Riley, Shawn J., Stephen Daniel DeGloria, and Robert Elliot, "A Terrain Ruggedness Index That Quantifies Topographic Heterogeneity," *Intermountain Journal of Sciences* 5:1-4 (1999), 23-27.

[25] Sundberg, Ralph, and Erik Melander, "Introducing the UCDP Georeferenced Event Dataset," *Journal of Peace Research* 50:4 (2013), 523-532.

[26] U.S. Geological Survey, Mineral Resources Data System, mrdata/usgs.gov/mrds (2005).

[27] Vicente-Serrano Sergio M., Santiago Beguería, J. Ignacio López-Moreno, Marta Angulo, and Ahmed M. El Kenawy, "A Global 0.5 Gridded Dataset (1901-2006) of a Multiscalar Drought Index Considering the Joint Effects of Precipitation and Temperature," *Journal of Hydrometeorology* 11:4 (2010), 1033-1043.

[28] Vicente-Serrano, Sergio M., Santiago Beguería, Jorge Lorenzo-Lacruz, Jesús Julio Camarero, Juan I. López-Moreno, Cesar Azorin-Molina, Jesús Revuelto, Enrique Morán-Tejeda, and Arturo Sanchez-Lorenzo, "Performance of Drought Indices for Ecological, Agricultural, and Hydrological Applications," *Earth Interactions* 16:10 (2012), 1-27.

[29] Weidmann, Nils B., Jan Ketil Rød, and Lars-Erik Cederman, "Representing Ethnic Groups in Space: A New Dataset," *Journal of Peace Research* 47:4 (2010), 491-499.

[30] Wucherpfennig, Julian, Nils B. Weidmann, Luc Girardin, Lars-Erik Cederman, and Andreas Wimmer, "Politically Relevant Ethnic Groups across Space and Time: Introducing the GeoEPR Dataset," *Conflict Management and Peace Science* 28 (2011), 423-437.

[31] Yu, Jihai, Robert de Jong, and Lung-fei Lee, "Quasi-maximum Likelihood Estimators for Spatial Dynamic Panel Data with Fixed Effects When Both N and T Are Large," *Journal of Econometrics* 146 (2008), 118–134.

Table A1: Summary Statistics, Cross-Sectional Sample

	No. Obs.	Mean	Std. Dev.
Fraction of years with conflict	2681	0.170	0.251
Shared	2681	0.382	0.486
Border	2681	0.036	0.186
Area, in km²	2681	10806.5	2522.6
Elevation, in m	2681	594.4	431.6
Rough, in m	2681	60.5	61.4
Distance to river, in km	2681	470.9	402.8
Road	2681	0.379	0.485
Minerals	2681	0.207	0.406
ELF	2681	0.193	0.234

Notes: Each observation is a cell.

Table A2: Conflict Incidence, Cross Section

Dependent variable: fraction of years over sample period with at least one conflict event

	(1)	(2)	(3)	(4)	(5)	(6)
	Model I, OLS		Model II, OLS		Model III, MLE	
W·Y					0.0943***	0.0658***
					(0.00223)	(0.00331)
Elevation [(a)]	0.041	0.06**	0.0986*	0.101**	0.103***	0.107***
	(0.027)	(0.0268)	(0.0526)	(0.0407)	(0.035)	(0.0351)
Rough [(a)]	0.341**	0.298*	0.132	0.153	0.179	0.168
	(0.158)	(0.177)	(0.181)	(0.163)	(0.141)	(0.145)
Area [(a)]	0.00326	-0.00516*	-0.00128	0.00099	-0.000673	0.000279
	(0.00349)	(0.00282)	(0.00387)	(0.00378)	(0.0032)	(0.00351)
Road	0.130***	0.123***	0.105***	0.0956***	0.0962***	0.0932***
	(0.0162)	(0.0117)	(0.0111)	(0.0104)	(0.0103)	(0.0101)
Distance to river [(a)]	-0.0529***	-0.0148	0.0204	-0.225***	-0.037	-0.155**
	(0.0198)	(0.0252)	(0.0822)	(0.0843)	(0.0468)	(0.0719)
Shared	0.0620***	0.0407***	0.0511***	0.0402***	0.0473***	0.0427***
	(0.0160)	(0.0121)	(0.0117)	(0.0108)	(0.00936)	(0.00912)
Border	-0.109***	-0.0747***	-0.0504**	-0.0545**	-0.0664***	-0.0635***
	(0.0198)	(0.0213)	(0.0225)	(0.0270)	(0.0199)	(0.0198)
Minerals	0.0552***	0.0616***	0.0512***	0.0515***	0.0494***	0.0486***
	(0.0156)	(0.0129)	(0.0109)	(0.0112)	(0.0105)	(0.0100)
ELF	0.0832**	0.0614**	0.0186	0.0198	0.0139	0.0179
	(0.0348)	(0.0266)	(0.0235)	(0.0235)	(0.0222)	(0.0215)
W·Elevation [(a)]			-0.0093	-0.00661	-0.0124***	-0.0112*
			(0.00724)	(0.00681)	(0.00479)	(0.00573)
W·Rough [(a)]			0.0286	0.0155	-0.017	-0.00886
			(0.0316)	(0.0395)	(0.0235)	(0.0284)
W·Area [(a)]			0.000695	-0.00114	-0.000121	-0.000816
			(0.000951)	(0.000973)	(0.000499)	(0.000688)
W·Road			0.00654*	0.00803**	-0.00571***	-0.00135
			(0.00359)	(0.00319)	(0.00205)	(0.00266)
W·Distance to river [(a)]			-0.0069	0.0346***	0.00385	0.0236**
			(0.0105)	(0.0119)	(0.006)	(0.0097)
W·Shared			0.00450	0.00188	-0.00231	-0.00183
			(0.00425)	(0.00312)	(0.00219)	(0.00236)
W·Border			-0.0149**	-0.00500	0.00313	0.00315
			(0.00734)	(0.00658)	(0.00462)	(0.00465)
W·Minerals			-0.000306	0.00884**	-0.00482*	0.00160
			(0.00462)	(0.00404)	(0.00267)	(0.00327)
W·ELF			0.0189**	0.0159**	0.00370	0.00643
			(0.00937)	(0.00718)	(0.00457)	(0.00516)
Observations	2,681	2,681	2,681	2,681	2,681	2,681
Country FE		X		X		X

Notes: Each observation is a cell. [(a)] Coefficient and standard error multiplied by 10^3. Standard errors in parenthesis corrected for spatial dependence, following Hsiang (2010). *** p<0.01, ** p<0.05, * p<0.1. W = binary contiguity matrix, cutoff 180 km.

Table A3: Different Types of Conflict Events, Cross Section

Dependent variable: fraction of years over sample period with at least one event

	Y = BATTLE	*Y = CIVILIAN*	*Y = RIOT*	*Y = REBEL*
	(1)	(2)	(3)	(4)
W·Y	0.0686***	0.0652***	0.0377***	0.0559***
	(0.00316)	(0.00330)	(0.00426)	(0.00362)
Elevation [(a)]	0.0903***	0.0773***	0.0515**	0.0227*
	(0.0255)	(0.0271)	(0.0243)	(0.0119)
Rough [(a)]	0.0074	0.1410	-0.0585	0.00116
	(0.0968)	(0.107)	(0.11)	(0.0472)
Area [(a)]	0.0015	0.0012	-0.0018	-0.00130
	(0.00223)	(0.00255)	(0.00289)	(0.00111)
Road	0.0437***	0.0599***	0.0628***	17.90***
	(0.00731)	(0.00784)	(0.00703)	(3.575)
Distance to river [(a)]	-0.0563	-0.0863	-0.124**	-0.0519**
	(0.0419)	(0.0526)	(0.0557)	(0.0247)
Shared	0.0256***	0.0268***	0.0105	0.0106***
	(0.00636)	(0.00685)	(0.00660)	(0.00351)
Border	-0.0405***	-0.0488***	-0.0378***	-0.0131
	(0.0145)	(0.0150)	(0.0140)	(0.0102)
Minerals	0.0298***	0.0268***	0.0232***	0.00432
	(0.00704)	(0.00771)	(0.00768)	(0.00347)
ELF	0.0204	0.0278*	0.0144	0.00222
	(0.0146)	(0.0157)	(0.0155)	(0.00724)
W·Elevation [(a)]	-0.0109***	-0.00703	-0.00086	-0.00254
	(0.00414)	(0.00453)	(0.00417)	(0.00192)
W·Rough [(a)]	0.0091	-0.0017	0.0196	-0.00349
	(0.0193)	(0.0209)	(0.0211)	(0.00913)
W·Area [(a)]	-0.000696	-0.000846	-0.001*	-2.77e-05
	(0.00045)	(0.000558)	(0.000553)	(0.000228)
W·Road	-0.000741	-0.00134	-0.00127	0.607
	(0.00173)	(0.00192)	(0.00163)	(0.899)
W·Distance to river [(a)]	0.010*	0.0132*	0.0172**	0.00946***
	(0.00581)	(0.00713)	(0.00732)	(0.00346)
W·Shared	-0.00119	-0.00132	-0.00128	0.000226
	(0.00166)	(0.00179)	(0.00173)	(0.000928)
W·Border	0.00166	0.00353	0.00607*	-0.000780
	(0.00329)	(0.00346)	(0.00345)	(0.00232)
W·Minerals	0.000625	0.00130	0.00607**	0.000941
	(0.00196)	(0.00239)	(0.00264)	(0.00104)
W·ELF	0.00524	0.00378	-0.00284	0.00218
	(0.00373)	(0.00376)	(0.00358)	(0.00178)
Observations	2,681	2,681	2,681	2,681
Country FE	X	X	X	X

Notes: Each observation is a cell. [(a)] Coefficient and standard error multiplied by 10^3. Standard errors in parenthesis corrected for spatial dependence, following Hsiang (2010). *** p<0.01, ** p<0.05, * p<0.1. W = binary contiguity matrix, cutoff 180 km.

Table A4: Conflict Incidence and Climate, Panel, Instrumental Variables Approach

Y= ANY EVENT. Dependent variable:	*Y*	*W·Y*	Y_{t-1}	*Y*	*W·Y*	Y_{t-1}	*Y*
	(1)	(2)	(3)	(4)	(5)	(6)	(7)
	OLS	1st Stage OLS	1st Stage OLS	IV	1st Stage OLS	1st Stage OLS	IV
Y_{t-1}	0.304***			0.750***			0.521***
	(0.0119)			(0.0255)			(0.0940)
W·Y	0.0641***			0.0561***			0.156***
	(0.00216)			(0.00391)			(0.0393)
SPEI	-0.00767	0.0904	0.0237*	-0.0217	0.183**	0.0291**	-0.0308*
	(0.0129)	(0.0601)	(0.0132)	(0.0142)	(0.0714)	(0.0135)	(0.0159)
$SPEI,_{t-1}$	0.0169	0.0154	-0.00153	0.0128	0.0335	0.000870	0.0101
	(0.0140)	(0.0544)	(0.0142)	(0.0164)	(0.0638)	(0.0144)	(0.0163)
$SPEI,_{t-2}$	-0.00849	0.0872*	0.00506	-0.0121	0.0818	0.00507	-0.0206
	(0.0135)	(0.0517)	(0.0134)	(0.0147)	(0.0640)	(0.0133)	(0.0158)
SPEI Growing Season	0.00493	-0.0943*	0.0111	0.00265	-0.0884	0.0117	0.0134
	(0.0136)	(0.0564)	(0.0146)	(0.0148)	(0.0665)	(0.0147)	(0.0160)
SPEI Growing Season, $_{t-1}$	-0.0463***	0.0846	-0.0112	-0.0402**	0.0529	-0.0108	-0.0494***
	(0.0154)	(0.0565)	(0.0151)	(0.0176)	(0.0623)	(0.0151)	(0.0171)
SPEI Growing Season, $_{t-2}$	-0.0126	-0.0226	-0.0249*	-0.000799	-0.0253	-0.0286**	-0.00365
	(0.0155)	(0.0553)	(0.0146)	(0.0171)	(0.0678)	(0.0145)	(0.0177)
W · SPEI	0.00254	0.000795	-0.00242	0.00306	-0.0349***	-0.00288	0.00169
	(0.00199)	(0.00891)	(0.00203)	(0.00219)	(0.0133)	(0.00265)	(0.00236)
W · SPEI, $_{t-1}$	-0.00280	0.00285	0.00238	-0.00397	0.000979	0.00156	-0.00436*
	(0.00214)	(0.00809)	(0.00215)	(0.00251)	(0.0119)	(0.00294)	(0.00248)
W · SPEI, $_{t-2}$	0.00206	-0.00265	-0.000640	0.00229	0.0202	-0.00318	0.00238
	(0.00205)	(0.00778)	(0.00206)	(0.00225)	(0.0130)	(0.00264)	(0.00232)
W · SPEI Growing Season	-0.00251	-0.00526	-0.00309	-9.06e-05	0.00476	-0.00418	0.00157
	(0.00232)	(0.00920)	(0.00243)	(0.00247)	(0.0164)	(0.00350)	(0.00269)
W · SPEI Growing Season, $_{t-1}$	0.00601**	-0.0274***	0.000186	0.00705**	-0.0248*	-0.00247	0.0113***
	(0.00261)	(0.00886)	(0.00249)	(0.00296)	(0.0144)	(0.00357)	(0.00328)
W · SPEI Growing Season, $_{t-2}$	0.000836	-0.0195**	-0.000413	0.00187	-0.0365**	0.00711**	0.00422
	(0.00256)	(0.00913)	(0.00243)	(0.00286)	(0.0165)	(0.00339)	(0.00311)
Y_{t-2}		0.502***	0.348***		0.842***	0.370***	
		(0.0339)	(0.0116)		(0.0422)	(0.0116)	
W·W·Y		0.317***	0.0204***				
		(0.00596)	(0.00116)				
W·W · SPEI					0.0240***	0.000564	
					(0.00454)	(0.000937)	
W·W · SPEI, $_{t-1}$					0.00594	0.000532	
					(0.00421)	(0.00105)	
W·W · SPEI, $_{t-2}$					-0.0110**	0.00182*	
					(0.00471)	(0.000981)	
W·W · SPEI Growing Season					-0.0200***	-0.000246	
					(0.00734)	(0.00153)	
W·W · SPEI Growing Season, $_{t-1}$					-0.0130*	0.000882	
					(0.00668)	(0.00159)	
W·W · SPEI Growing Season, $_{t-2}$					0.00598	-0.00490***	
					(0.00681)	(0.00151)	
Observations	32,526	32,526	32,526	32,526	32,526	32,526	32,526
Angrist-Pischke F statistic		2019.28	713.00		7.96	30.95	

Notes: Each observation is a cell/year. Standard errors in parenthesis corrected for clustering at the cell level. Angrist-Pischke first-stage statistics reported. All regressions include the controls and fixed effects of the specification in Table 2, column 3. *** p<0.01, ** p<0.05, * p<0.1. W = binary contiguity matrix, cutoff 180 km.

Table A5: Climate and Conflict Projections

	Mean	Std. Dev.	Correlation with Benchmark Model
A: Average projected SPEI Growing Season, 2016-2050			
FGOALS_g2_rcp26 (benchmark)	-0.135	0.184	
FGOALS_g2_rcp45	-0.130	0.181	0.973***
FGOALS_g2_rcp85	-0.116	0.187	0.914***
EC_EARTH_rcp26	-0.106	0.164	0.950***
EC_EARTH_rcp45	-0.107	0.173	0.952***
EC_EARTH_rcp85	-0.096	0.184	0.912***
FIO_ESM_rcp26	-0.115	0.169	0.883***
FIO_ESM_rcp45	-0.108	0.174	0.936***
FIO_ESM_rcp60	-0.116	0.182	0.931***
FIO_ESM_rcp85	-0.082	0.184	0.893***
B: Average marginal impact of projected SPEI Growing Season on conflict, 2016-2050, Model III			
FGOALS_g2_rcp26 (benchmark)	0.012	0.012	
FGOALS_g2_rcp45	0.007	0.015	0.583***
FGOALS_g2_rcp85	0.007	0.013	0.631***
EC_EARTH_rcp26	0.009	0.015	0.721***
EC_EARTH_rcp45	0.009	0.018	0.707***
EC_EARTH_rcp85	0.005	0.016	0.664***
FIO_ESM_rcp26	0.007	0.017	0.528***
FIO_ESM_rcp45	0.005	0.013	0.468***
FIO_ESM_rcp60	0.007	0.015	0.629***
FIO_ESM_rcp85	0.009	0.019	0.650***
C: Average marginal impact of projected SPEI Growing Season on conflict, 2016-2050, Model I			
FGOALS_g2_rcp26 (benchmark)	0.012	0.021	
FGOALS_g2_rcp45	0.012	0.021	0.674***
FGOALS_g2_rcp85	0.010	0.021	0.608***
EC_EARTH_rcp26	0.010	0.020	0.596***
EC_EARTH_rcp45	0.010	0.021	0.632***
EC_EARTH_rcp85	0.008	0.021	0.610***
FIO_ESM_rcp26	0.010	0.020	0.582***
FIO_ESM_rcp45	0.010	0.020	0.633***
FIO_ESM_rcp60	0.010	0.021	0.627***
FIO_ESM_rcp85	0.007	0.021	0.614***

Each row corresponds to a climate projections model. Panel A: projected SPEI Growing Season, 2016-2050. Panel B: estimated marginal impact of projected SPEI Growing Season on conflict incidence, 2016-2050, according to model III estimates from Table 2, column 5. Panel C: estimated marginal impact of projected SPEI Growing Season on conflict incidence, averaged over 2016-2050, according to model I estimates from Table 2, column 1. *** p<0.01, ** p<0.05, * p<0.1.

Table A6: Heterogeneous Spatial Decay of Agricultural Shocks, Panel

Dependent variable (Y)=1 if conflict event in year t (ANY EVENT)

	(1)	(2)	(3)	(4)
Neighbors included in W_1	Same Main Group	Same Main Crop	Same Main Crop and Same Main Group	Different Main Crop Same Main Group
Neighbors included in W_2	Different Main Group	Different Main Crop	Same Main Crop and Different Main Group	Different Main Crop and Different Main Group
W_1 · *SPEI Growing Season*	-0.00485*	-0.00594*	-0.00515	-0.00542
	(0.00290)	(0.00333)	(0.00495)	(0.00376)
W_1 · *SPEI Growing Season*, $_{t-1}$	0.00601**	0.00269	0.0119**	0.000661
	(0.00295)	(0.00316)	(0.00523)	(0.00356)
W_1 · *SPEI Growing Season*, $_{t-2}$	-0.00134	0.00165	-0.000847	-0.000749
	(0.00300)	(0.00333)	(0.00508)	(0.00372)
W_2 · *SPEI Growing Season*	-0.00403	-0.00204	0.00413	-0.00841
	(0.00437)	(0.00360)	(0.00689)	(0.00529)
W_2 · *SPEI Growing Season*, $_{t-1}$	0.00928**	0.0115***	0.0106	0.00376
	(0.00406)	(0.00380)	(0.00652)	(0.00495)
W_2 · *SPEI Growing Season*, $_{t-2}$	0.00216	-0.00109	-0.00551	0.00550
	(0.00424)	(0.00385)	(0.00725)	(0.00516)
Observations				
Country x Year FE	X	X	X	X
Cell FE	X	X	X	X

Notes: Each observation is a cell/year. Estimation by MLE. Standard errors in parenthesis corrected for clustering at the cell level. *** p<0.01, ** p<0.05, * p<0.1.

Table A7: Onset and Termination, Panel

	Onset					Termination
Dependent variable:	*Y = ANY_EVENT*	*Y = BATTLE*	*Y = CIVILIAN*	*Y = RIOT*	*Y = REBEL*	*Y = ANY_EVENT*
	(1)	(2)	(3)	(4)	(5)	(6)
SPEI	-0.00359	0.0101	-0.0154*	-0.00378	-0.00496	0.0570
	(0.0116)	(0.00896)	(0.00899)	(0.00765)	(0.00523)	(0.0553)
SPEI, $_{t-1}$	0.0165	-0.00184	0.0178**	0.0149*	0.0129**	0.137***
	(0.0119)	(0.00946)	(0.00904)	(0.00821)	(0.00598)	(0.0503)
SPEI, $_{t-2}$	-0.00361	0.00358	0.00712	-0.00928	-0.00586	-0.0141
	(0.0114)	(0.00897)	(0.00898)	(0.00747)	(0.00570)	(0.0473)
SPEI Growing Season	0.0103	0.00961	0.0152*	0.0158**	0.00392	0.00659
	(0.0114)	(0.00922)	(0.00901)	(0.00798)	(0.00563)	(0.0537)
SPEI Growing Season, $_{t-1}$	-0.0370***	-0.0317***	-0.0393***	-0.0144	-0.0163***	-0.0186
	(0.0123)	(0.0102)	(0.0103)	(0.00897)	(0.00624)	(0.0489)
SPEI Growing Season, $_{t-2}$	-0.00436	-0.00571	-0.00501	0.00988	0.00842	0.0585
	(0.0126)	(0.0100)	(0.00959)	(0.00884)	(0.00589)	(0.0488)
W · SPEI	0.000107	-0.00263*	0.00287*	0.000917	0.000542	0.00267
	(0.00195)	(0.00153)	(0.00154)	(0.00117)	(0.000834)	(0.00946)
W · SPEI, $_{t-1}$	-0.00408**	-0.000511	-0.00361**	-0.00127	-0.00204**	-0.0249***
	(0.00204)	(0.00165)	(0.00155)	(0.00136)	(0.000958)	(0.00912)
W · SPEI, $_{t-2}$	0.00246	-0.000136	0.000258	0.00202*	0.00102	0.00312
	(0.00194)	(0.00157)	(0.00154)	(0.00119)	(0.000948)	(0.00845)
W · SPEI Growing Season	-0.00328	-0.00318*	-0.00555***	-0.000949	0.000174	-0.0119
	(0.00221)	(0.00179)	(0.00176)	(0.00128)	(0.00104)	(0.0104)
W · SPEI Growing Season, $_{t-1}$	0.00694***	0.00536***	0.00595***	0.000871	0.00178*	0.00226
	(0.00234)	(0.00193)	(0.00193)	(0.00157)	(0.00105)	(0.0102)
W · SPEI Growing Season, $_{t-2}$	-0.000709	0.00192	0.000417	-0.00294**	-0.00203*	-0.0237**
	(0.00233)	(0.00189)	(0.00179)	(0.00143)	(0.00110)	(0.00984)
Observations	33,687	35,654	35,588	36,560	37,530	6,355
Country x Year FE	X	X	X	X	X	X
Cell FE	X	X	X	X	X	X

Notes: Each observation is a cell/year. Estimation by OLS. Standard errors in parenthesis corrected for spatial and serial correlation according to Hsiang (2010). *** p<0.01, ** p<0.05, * p<0.1. W = binary contiguity matrix, cutoff 180 km.

Table A8: Sensitivity to Different Spatial Resolutions

Dependent variable (Y)=1 if conflict event in year t (ANY EVENT)

	(1)	(2)	(3)	(4)	(5)
	0.5 X 0.5 Degree	2x2 Degree			
		Panel I	Panel II	Panel III	Panel IV
Y_{t-1}	0.126***	0.0983***	0.117***	0.110***	0.133***
	(0.00676)	(0.0140)	(0.0140)	(0.0141)	(0.0139)
W·Y	0.0217***	0.00243	0.000689	0.00175	0.00224
	(0.00102)	(0.00275)	(0.00264)	(0.00277)	(0.00279)
SPEI	-0.0111	-0.00973	0.0401*	0.0262	-0.0240
	(0.0111)	(0.0223)	(0.0218)	(0.0239)	(0.0247)
SPEI, $_{t-1}$	-0.00458	0.00521	-0.0243	-0.0143	-0.0284
	(0.0114)	(0.0218)	(0.0223)	(0.0226)	(0.0225)
SPEI, $_{t-2}$	0.0144	0.0339	0.0377*	0.0120	-0.000402
	(0.0111)	(0.0231)	(0.0214)	(0.0233)	(0.0229)
SPEI Growing Season	0.00979	0.0186	0.00205	0.00451	0.0102
	(0.00968)	(0.0326)	(0.0323)	(0.0331)	(0.0326)
SPEI Growing Season, $_{t-1}$	0.00745	0.0106	0.0280	0.00476	0.0387
	(0.0102)	(0.0314)	(0.0323)	(0.0329)	(0.0301)
SPEI Growing Season, $_{t-2}$	-0.00769	-0.0711**	-0.0466	2.28e-05	-0.00942
	(0.0102)	(0.0328)	(0.0322)	(0.0322)	(0.0311)
W · SPEI	0.00193	-0.000597	-0.0127***	-0.00757	0.00328
	(0.00172)	(0.00485)	(0.00464)	(0.00492)	(0.00513)
W · SPEI, $_{t-1}$	-0.000265	-0.00422	1.46e-05	-0.00527	-0.000113
	(0.00175)	(0.00497)	(0.00456)	(0.00466)	(0.00490)
W · SPEI, $_{t-2}$	-0.00281	-0.00541	-0.00396	-0.00158	0.000882
	(0.00172)	(0.00482)	(0.00472)	(0.00493)	(0.00507)
W · SPEI Growing Season	-0.00279*	0.00503	0.00808	0.00769	0.00174
	(0.00161)	(0.00727)	(0.00787)	(0.00739)	(0.00713)
W · SPEI Growing Season, $_{t-1}$	9.83e-05	-0.00538	-0.00425	-0.00208	-0.0101
	(0.00171)	(0.00765)	(0.00740)	(0.00744)	(0.00719)
W · SPEI Growing Season, $_{t-2}$	0.00246	0.0113	0.00554	-0.00381	-0.000871
	(0.00169)	(0.00756)	(0.00769)	(0.00763)	(0.00807)
Observations	83,972	9,856	9,884	9,758	9,856
Country x Year FE	X	X	X	X	X
Cell FE	X	X	X	X	X

Notes: Each observation is a cell/year. Estimation by MLE. Standard errors in parenthesis corrected for clustering at the cell level. *** p<0.01, ** p<0.05, * p<0.1. Column 1: W= binary contiguity matrix, cutoff 90 km. Columns 2-5: W = binary contiguity matrix, cutoff 390 km.

Table A9: Sensitivity to Different Spatial Matrices

Dependent variable (Y)=1 if conflict event in year t (ANY EVENT)

	(1)	(2)	(3)	(4)	(5)	(6)
Weighting matrix	Binary, cutoff:			Inverse distance, cutoff:		
	290km	450km	600km	290km	450km	600km
Y_{t-1}	0.119***	0.120***	0.121***	0.118***	0.118***	0.119***
	(0.00846)	(0.00848)	(0.00837)	(0.00845)	(0.00844)	(0.00840)
$W{\cdot}Y$	0.0120***	0.00413***	0.000621	2.181***	1.436***	0.814***
	(0.000920)	(0.000602)	(0.000467)	(0.151)	(0.132)	(0.125)
SPEI	-0.00672	-0.000478	0.00145	-0.00628	-0.00172	0.000372
	(0.0105)	(0.00829)	(0.00731)	(0.0114)	(0.00961)	(0.00877)
$SPEI,_{t-1}$	0.00823	-0.00195	-0.00940	0.0105	0.00514	0.00206
	(0.0105)	(0.00812)	(0.00700)	(0.0114)	(0.00954)	(0.00861)
$SPEI,_{t-2}$	-0.00340	0.000348	0.00429	-0.00701	-0.00274	0.00136
	(0.0103)	(0.00814)	(0.00720)	(0.0112)	(0.00945)	(0.00864)
SPEI Growing Season	0.0115	-0.000522	-0.00352	0.0132	0.00517	0.000771
	(0.0120)	(0.0110)	(0.0103)	(0.0124)	(0.0116)	(0.0112)
SPEI Growing Season, $_{t-1}$	-0.0263**	-0.0135	-0.00200	-0.0295**	-0.0205*	-0.0104
	(0.0128)	(0.0113)	(0.0103)	(0.0134)	(0.0124)	(0.0118)
SPEI Growing Season, $_{t-2}$	-0.0136	-0.0164	-0.0127	-0.0111	-0.0150	-0.0151
	(0.0130)	(0.0114)	(0.0105)	(0.0136)	(0.0125)	(0.0119)
$W \cdot SPEI$	0.000101	-0.000328	-0.000656**	0.00993	-0.0561	-0.0949
	(0.000857)	(0.000384)	(0.000289)	(0.150)	(0.0961)	(0.0849)
$W \cdot SPEI,_{t-1}$	-0.00175**	-0.000784**	-0.000472*	-0.303**	-0.205**	-0.198**
	(0.000862)	(0.000377)	(0.000283)	(0.152)	(0.0965)	(0.0858)
$W \cdot SPEI,_{t-2}$	0.000604	2.60e-06	-0.000177	0.164	0.0594	0.00371
	(0.000846)	(0.000371)	(0.000275)	(0.149)	(0.0943)	(0.0824)
W · SPEI Growing Season	-0.00125	-0.000369	-0.000221	-0.226	-0.101	-0.0895
	(0.00113)	(0.000596)	(0.000493)	(0.194)	(0.140)	(0.133)
W · SPEI Growing Season, $_{t-1}$	0.00198*	0.000409	-0.000345	0.378*	0.171	0.0599
	(0.00117)	(0.000595)	(0.000470)	(0.203)	(0.144)	(0.134)
W · SPEI Growing Season, $_{t-2}$	0.000836	0.000769	0.000166	0.0798	0.123	0.120
	(0.00120)	(0.000617)	(0.000474)	(0.209)	(0.149)	(0.137)
Observations	35,042	35,042	35,042	35,042	35,042	35,042
Country x Year FE	X	X	X	X	X	X
Cell FE	X	X	X	X	X	X

Notes: Each observation is a cell/year. Estimation by MLE. Standard errors in parenthesis corrected for clustering at the cell level. *** p<0.01, ** p<0.05, * p<0.1.

Table A10: Other Climate Indicators

Dependent variable (Y)=1 if conflict event in year t (ANY EVENT)

	(1)	(2)	(3)	(4)	(5)	(6)
	SPEI Annual	SPEI Shock	SPEI Growing Season	Weighted SPEI	Log Rain	Temperature
Y_{t-1}	0.121***	0.121***	0.121***	0.124***	0.121***	0.121***
	(0.00849)	(0.00850)	(0.00849)	(0.0102)	(0.00851)	(0.00848)
W·Y	0.0228***	0.0228***	0.0228***	0.0193***	0.0229***	0.0227***
	(0.00150)	(0.00150)	(0.00150)	(0.00199)	(0.00151)	(0.00151)
Climate, Growing Season Indicator		-0.00471	0.0204	0.0131	-0.00117	-0.00895
		(0.0190)	(0.0133)	(0.0286)	(0.00270)	(0.0191)
Climate, Growing Season Indicator, $_{t-1}$		0.0289	-0.0384***	-0.0182	-0.000390	0.0334
		(0.0189)	(0.0139)	(0.0274)	(0.00359)	(0.0205)
Climate, Growing Season Indicator, $_{t-2}$		0.0140	-0.00865	-0.0321	-0.00388	-0.0162
		(0.0188)	(0.0140)	(0.0270)	(0.00335)	(0.0185)
Climate, Growing Season Indicator (sq.)			-0.00494			
			(0.0128)			
Climate, Growing Season Indicator, $_{t-1}$ *(sq.)*			-0.0118			
			(0.0141)			
Climate, Growing Season Indicator, $_{t-2}$ *(sq.)*			0.00706			
			(0.0139)			
Climate	0.00640	0.00545	-0.00499	-0.0216*	0.000484	-0.00245
	(0.0120)	(0.0123)	(0.0132)	(0.0131)	(0.000643)	(0.0201)
Climate, $_{t-1}$	-0.00395	0.000828	0.0155	-0.000457	-0.000179	-0.0188
	(0.0115)	(0.0118)	(0.0130)	(0.0129)	(0.000572)	(0.0199)
Climate, $_{t-2}$	-0.0179	-0.0158	-0.0149	-0.00342	0.00110	0.0351*
	(0.0116)	(0.0119)	(0.0126)	(0.0131)	(0.000734)	(0.0194)
W · Climate, Growing Season Indicator		-0.000555	-0.00443*	-0.00809	1.53e-05	0.00789**
		(0.00375)	(0.00257)	(0.00536)	(0.000942)	(0.00362)
W · Climate, Growing Season Indicator, $_{t-1}$		-0.00610*	0.00658**	-0.00179	0.000596	-0.00124
		(0.00364)	(0.00257)	(0.00521)	(0.000847)	(0.00382)
W · Climate, Growing Season Indicator, $_{t-2}$		3.57e-05	0.000594	0.00523	0.000241	0.00489
		(0.00370)	(0.00262)	(0.00521)	(0.000986)	(0.00358)
W · Climate, Growing Season Indicator (sq.)			-0.000777			
			(0.00239)			
W · Climate, Growing Season Indicator, $_{t-1}$ *(sq.)*			-0.000149			
			(0.00256)			
W · Climate, Growing Season Indicator, $_{t-2}$ *(sq.)*			-0.000386			
			(0.00275)			
W · Climate	-0.00222	-0.00230	0.000105	0.00439*	0.000368***	0.000745
	(0.00192)	(0.00202)	(0.00220)	(0.00228)	(0.000135)	(0.00315)
W · Climate, $_{t-1}$	-0.00122	-0.00226	-0.00460**	-0.000353	1.90e-07	0.00247
	(0.00186)	(0.00196)	(0.00218)	(0.00229)	(0.000146)	(0.00321)
W · Climate, $_{t-2}$	0.00336*	0.00334*	0.00330	0.00171	0.000113	-0.00683**
	(0.00187)	(0.00196)	(0.00211)	(0.00230)	(0.000163)	(0.00312)
Observations	35,042	35,042	35,042	25,508	35,042	35,042
Country x Year FE	X	X	X	X	X	X
Cell FE	X	X	X	X	X	X

Notes: Each observation is a cell/year. Estimation by MLE. Standard errors in parenthesis corrected for clustering at the cell level. The averages of SPEI Shock, rainfall and temperature in the sample are respectively 0.106, 64.7 mm and 25.2 ºC.*** p<0.01, ** p<0.05, * p<0.1. W = binary contiguity matrix, cutoff 180 km.

Table A11: Alternative Conflict Data

Dependent variable (Y)=1 if GED conflict event in year t	(1)	(2)	(3)	(4)	(5)
	MODEL I OLS	MODEL II OLS	MODEL III MLE	MODEL III MLE	MODEL III MLE
Y_{t-1}			0.345***	0.353***	0.189***
			(0.0103)	(0.0104)	(0.0120)
$W{\cdot}Y$			0.0574***	0.0476***	0.0384***
			(0.00144)	(0.00155)	(0.00187)
SPEI	0.0191***	0.00131	0.00249	0.00243	0.00232
	(0.00561)	(0.0106)	(0.00914)	(0.00953)	(0.00938)
SPEI, $_{t-1}$	0.0107**	0.00960	0.00297	0.00705	0.00725
	(0.00533)	(0.0103)	(0.00966)	(0.0100)	(0.00985)
SPEI, $_{t-2}$	0.00879	0.0155	0.00942	0.00222	0.00200
	(0.00539)	(0.0108)	(0.00936)	(0.00969)	(0.00972)
SPEI Growing Season	-0.0223**	-0.0206	-0.0129	-0.0117	-0.00953
	(0.0107)	(0.0127)	(0.00984)	(0.00983)	(0.0116)
SPEI Growing Season, $_{t-1}$	-0.0329***	-0.0241*	-0.0151	-0.0141	-0.00997
	(0.0103)	(0.0132)	(0.0116)	(0.0116)	(0.0119)
SPEI Growing Season, $_{t-2}$	-0.0334***	-0.0120	-0.00631	-0.00357	0.00321
	(0.0104)	(0.0124)	(0.0111)	(0.0112)	(0.0107)
W · SPEI		0.00262	-0.000294	0.000163	-0.00257
		(0.00176)	(0.00136)	(0.00159)	(0.00163)
W · SPEI, $_{t-1}$		0.000464	0.000246	0.000575	-0.00171
		(0.00171)	(0.00145)	(0.00170)	(0.00171)
W · SPEI, $_{t-2}$		-0.000225	-0.000629	0.00111	-0.000278
		(0.00178)	(0.00142)	(0.00163)	(0.00171)
W · SPEI Growing Season		-0.000436	0.00147	-0.000353	0.00169
		(0.00242)	(0.00161)	(0.00185)	-0.00213
W · SPEI Growing Season, $_{t-1}$		-0.00199	-5.92e-05	-0.00133	0.000591
		(0.00247)	(0.00186)	(0.00215)	(0.00225)
W · SPEI Growing Season, $_{t-2}$		-0.00522**	-0.00104	-0.000131	9.87e-06
		(0.00225)	(0.00179)	(0.00205)	(0.00193)
Observations	35,042	35,042	35,042	35,042	35,042
Controls	X	X	X	X	
Year FE	X	X	X		
Country-specific linear time trend	X	X	X		
Country x Year FE				X	X
Cell FE					X

Notes: Each observation is a cell/year. Standard errors in parenthesis. Cols. 1,2 corrected for spatial and serial correlation following Hsiang (2010). Cols. 3-5 corrected for clustering at the cell level. *** p<0.01, ** p<0.05, * p<0.1. W = binary contiguity matrix, cutoff 180 km.

Table A12: Alternative Lags and Leads Structure, Panel

Dependent variable (Y)=1 if conflict event in year t (ANY EVENT)

	(1)	(2)	(3)
Y_{t-1}	0.121***	0.106***	0.0862***
	(0.00850)	(0.00907)	(0.0112)
W·Y	0.0228***	0.0212***	0.0166***
	(0.00150)	(0.00163)	(0.00194)
SPEI Growing Season, $_{t+4}$			-0.00540
			(0.0182)
SPEI Growing Season, $_{t+3}$			-0.00473
			(0.0191)
SPEI Growing Season, $_{t+2}$			0.00990
			(0.0186)
SPEI Growing Season, $_{t+1}$			0.0212
			(0.0176)
SPEI Growing Season	0.0204	0.0180	0.0175
	(0.0129)	(0.0141)	(0.0169)
SPEI Growing Season, $_{t-1}$	-0.0375***	-0.0409***	-0.0315*
	(0.0136)	(0.0152)	(0.0178)
SPEI Growing Season, $_{t-2}$		0.000585	-0.00851
		(0.0152)	(0.0195)
SPEI Growing Season, $_{t-3}$		-0.0275*	-0.0245
		(0.0153)	(0.0189)
SPEI Growing Season, $_{t-4}$		-0.0112	-0.0260
		(0.0161)	(0.0189)
W · SPEI Growing Season, $_{t+4}$			-0.00179
			(0.00337)
W · SPEI Growing Season, $_{t+3}$			0.00252
			(0.00353)
W · SPEI Growing Season, $_{t+2}$			-0.0118***
			(0.00350)
W · SPEI Growing Season, $_{t+1}$			-0.00856***
			(0.00325)
W · SPEI Growing Season	-0.00413*	-0.00349	-0.00513
	(0.00246)	(0.00271)	(0.00339)
W · SPEI Growing Season, $_{t-1}$	0.00644**	0.00637**	0.00795**
	(0.00252)	(0.00284)	(0.00336)
W · SPEI Growing Season, $_{t-2}$		-4.87e-05	-0.00262
		(0.00276)	(0.00351)
W · SPEI Growing Season, $_{t-3}$		0.00716**	0.00631*
		(0.00281)	(0.00356)
W · SPEI Growing Season, $_{t-4}$		0.00255	0.00499
		(0.00303)	(0.00374)
Observations	35,042	30,036	20,024
Country x Year FE	X	X	X
Cell FE	X	X	X

Each observation is a cell/year. Estimation by MLE. Standard errors in parenthesis corrected for spatial and temporal dependence, following Hsiang(2010). W = binary contiguity matrix, cutoff 180 km.

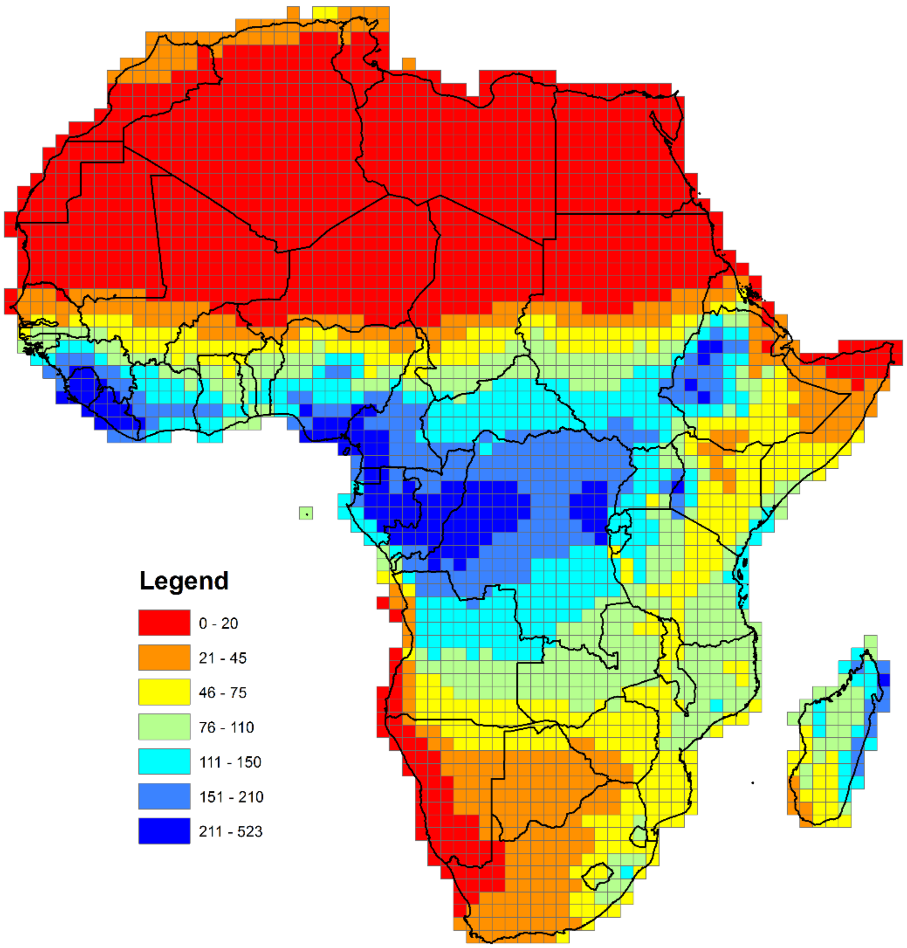

Figure A1:
Average Yearly Rainfall (in mm), 1997-2011

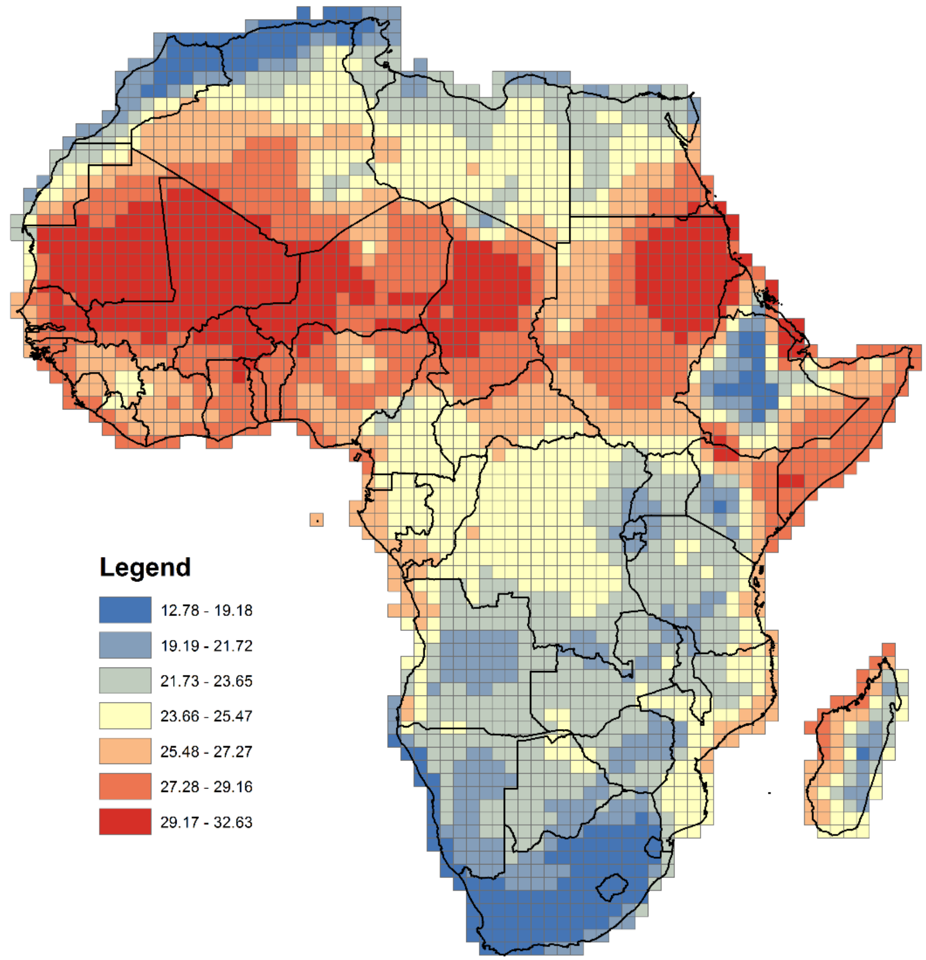

Figure A2:
Average Yearly Temperature (in °C), 1997-2011

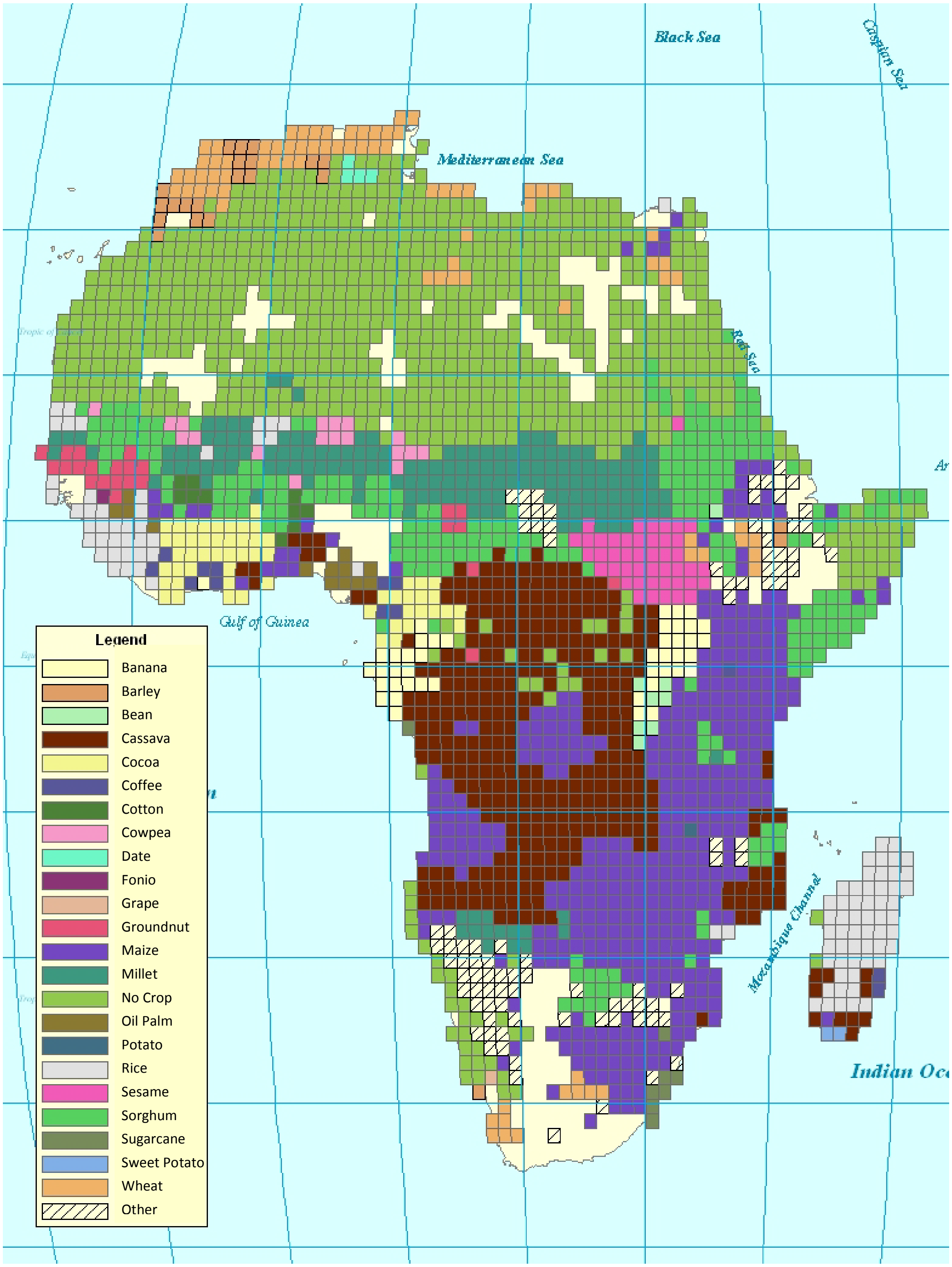

Figure A3:
Main Crop

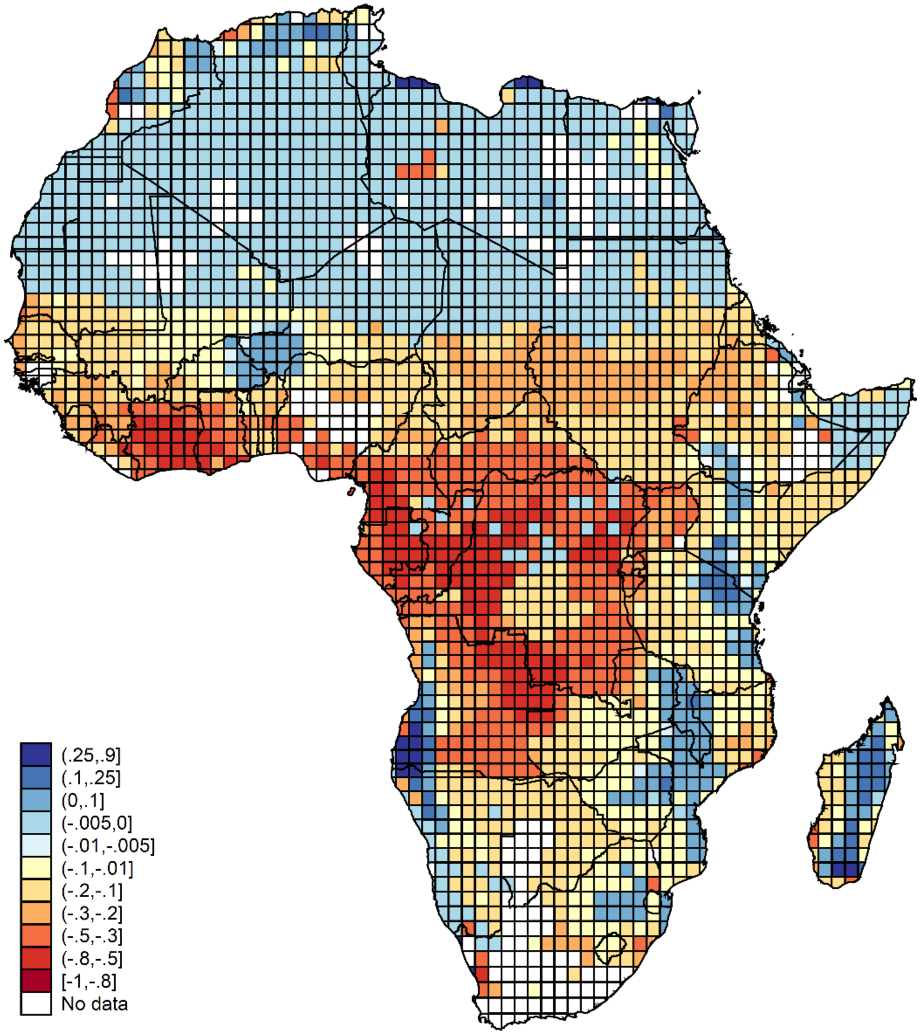

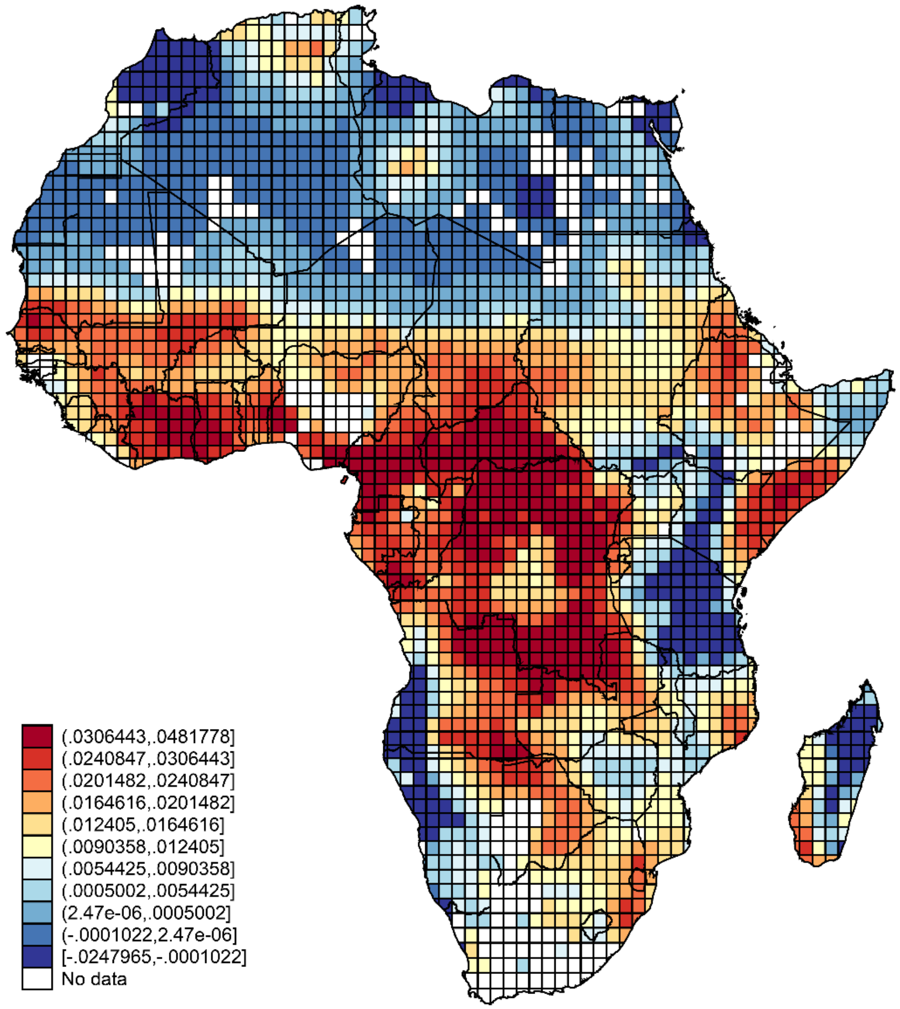

Figure A4:

Average Projected SPEI Growing Season, 2016-2050, FGOALS-RCP 2.6 Projections

Figure A5:

Average Marginal Effects of Projected SPEI Growing Season, 2016-2050, FGOALS-RCP 2.6 Projections